Bulletin of Earthquake Engineering
https://doi.org/10.1007/s10518-024-02016-6

ORIGINAL ARTICLE

Code-based brittle capacity models for seismic assessment of pre-code RC buildings: comparison and consequences on retrofit

Santa Anna Scala[1] · **Maria Teresa De Risi**[1] · **Gerardo Mario Verderame**[1]

Received: 13 May 2024 / Accepted: 4 September 2024

Abstract
The existing Reinforced Concrete (RC) buildings stock is often characterized by a significant seismic vulnerability, due to the absence of capacity design principles, even in regions with high seismic hazard, such as Italy. Approximately 67% of existing RC buildings in Italy have been designed without considering seismic actions (GLD), resulting in very low transverse reinforcement amount in beams and, particularly, in columns. Additionally, beam-column joints typically totally lack stirrups. Consequently, shear failures under seismic actions are very likely for this pre-code building typology, often limiting their seismic capacity. However, the assessment of shear failures in beams/columns or joints varies significantly from code to code worldwide. The main goal of this work is to quantify the impact of different code-based brittle capacity models on the seismic capacity assessment and retrofit, focusing on GLD Italian pre-1970 RC buildings. This comparative analysis is carried out by first considering three current codes, emphasizing their, even significant, differences: European (EN 1998-3-1. 2005), Italian (D.M. 2018), and American (ASCE SEI/41 2017) standards. Then, shear capacity models prescribed by the current drafts of the next generation of Eurocodes are implemented and compared to the current models. The assessment includes: (*i*) a parametric comparison among models; (*ii*) the evaluation of case-study buildings capacity in their as-built condition and after shear strengthening interventions. The latter is performed on 3D "bare" models, due to the lack of practical guidance in most codes on modelling masonry infills.

Keywords Brittle capacity models · Code-based assessment · RC buildings · Shear failures · Shear strengthening · Retrofitting design · Second-generation eurocodes

✉ Maria Teresa De Risi
mariateresa.derisi@unina.it

Santa Anna Scala
santaanna.scala@unina.it

Gerardo Mario Verderame
verderam@unina.it

[1] Department of Structures for Engineering and Architecture, University of Naples Federico II, via Claudio, 21, Napoli 80125, Italy

Published online: 16 September 2024

1 Introduction

Post-earthquake surveys worldwide have brought to light the significant impact of shear failures in beams, columns, or beam-column joints on the seismic performance of existing reinforced concrete (RC) buildings. Recent catastrophic seismic events (e.g., Verderame et al. 2014; Masi et al. 2019) have highlighted the detrimental effects of inadequate transverse reinforcements or the absence of seismic detailing, especially in joint regions and columns, on the structural response. Consequently, ensuring the accurate estimation of shear capacity is imperative for a comprehensive evaluation of the structural performance (Karakas et al., 2022; Lupoi et al. 2004) and the design of effective retrofitting strategies.

In the literature, a multitude of shear capacity models for existing beam-column elements have been formulated by means of an empirical approach. Several of these (Priestley et al. 1994; Sezen and Moehle 2004; Biskinis et al. 2004; Kowalsky and Priestley 2000) forecast a deterioration in shear strength under seismic cyclic loading as ductility demand rises. Nonetheless, despite being conceptually rooted in the same theory, these models exhibit significant differences. Shear resistance is primarily attributed to two factors: one associated with the presence of transverse reinforcements, and the other reliant on the concrete resisting mechanisms. Nevertheless, some models relegate the strength cyclic degradation to the concrete resisting contributions only (e.g, Priestley et al. 1994), owing to a progressive reduction in load-carrying capacity with crack propagation. Other models extend the shear strength degradation to the contribution of transverse reinforcement, considering the potential loss of anchorage and bond capacity of the reinforcement due to concrete cracking (Sezen and Moehle 2004; Biskinis et al. 2004). In addition, among the various capacity models, there is not unanimous agreement on the definition of resistance contributions, especially about the concrete strength contribution. For example, Sezen and Moehle (2004)'s model evaluates this contribution using the Mohr's circle approach including the influence of axial load. In contrast, Biskinis et al. (2004)' s model considers the axial load with an additional resistance contribution, not subjected to any cyclic degradation effect.

In addition to empirical capacity models, the shear strength of RC elements can be assessed through the application of the Modified Compression Field Theory (Vecchio and Collins 1986) or its simplified variants (Bentz et al. 2006; CSA Standard, 2006; Model Code, 2010; Marcantonio et al. 2015). This theory represents the latest advancement of an approach that originated in the early 1900s, according to which the shear strength of a RC element is governed by a truss mechanism (Ritter 1899; Morsch 1909) with compressive stresses inclined at 45° to the longitudinal axis of the element. This very first model neglected any contribution by the cracked concrete, potentially resulting in overly conservative estimates of shear strength for elements with limited transverse reinforcement. Moreover, studies from the 1980s revealed that the inclination angle is seldom exactly 45°. The necessity for a rational determination of this angle gave rise to the Compression Field Theory (CFT, Collins 1978), subsequently modified to consider the tensile stresses in the cracked concrete (MCFT, Vecchio and Collins 1986). The method estimates the inclination angle based on the strain distribution in the cross-section of the element and it has been suggested by the Model Code (2010) - with different levels of approximations (Model Code, 2010; Biskinis and Fardis 2020).

In last years, many experimental works have been conducted focusing on the estimation of the shear strength of beam-column joints without transverse reinforcement, which typi-

cally characterize existing buildings. Most of these studies focus on exterior joints (e.g., Vollum and Newman 1999; Pantelides et al. 2002; Tsnos, 2007), generally more vulnerable, identifying the parameters that can most significantly affect joint strength. Among these parameters, in addition to joint configuration (interior or exterior) and concrete compressive strength (Priestley 1997; Kim and LaFave 2012), the joint aspect ratio, the beam longitudinal reinforcement ratio (Park and Mosalam 2012), and the column axial load (Priestley 1997) were identified as key factors, as also confirmed by Jeon et al. (2014) based on a wide experimental dataset. Nevertheless, there is not a full consensus within the research community about the influence of some factors on the joint shear strength. For example, several studies acknowledge the influence of axial force only on the deformability of the joint and not on its strength (e.g. Fujii and Morita 1991; Park and Mosalam 2012). An increase in column axial load has not or limited influence on interior and exterior joints strength respectively, according to Fujii and Morita (1991). A detrimental effect on the joint shear strength due to high axial loads has been observed by Li et al. (2015).

The discrepancies among the different brittle capacity models proposed in the literature, both for beam/column elements and beam-column joints, have been integrated into various national standards (e.g., EN 1998-3, 2005; D.M. 2018; ASCE/SEI-41, 2017; NZS 3101, 2006), and, thus, the assessment of the seismic capacity of RC buildings is based on technical codes that rely on (often very) different capacity models.

This study aims at investigating the potential impact of using different code-based brittle capacity models first in terms of parametric comparison and, then, by applying them on the seismic assessment and retrofit of RC case-study buildings. This assessment is conducted through nonlinear static pushover analysis within the N2 framework (Fajfar 2000) on Italian pre-1970 ("pre-code") case-study buildings with different numbers of stories, in both the as-built condition and after the implementation of a retrofitting strategy that addresses brittle tensile-only failures (De Risi et al. 2023a). Three current code prescriptions are considered herein: the current Eurocode 8 (labelled "EC8 2005" in what follows) (EN 1998-3, 2005), Italian technical code D.M. (2018) (labelled "NTC 2018" hereinafter), and American standards "ASCE/SEI" (ASCE/SEI-41, 2017). Based on European and Italian codes (EC8 2005; NTC 2018) approach, the building capacity at the Severe Damage (SD) Limit State (LS) is always assessed as that corresponding to the first failure attained at that LS. It is worth noting that this choice of "failure" criterion is certainly conservative with respect to the "real" (sidesway or gravity load) collapse of a building (Shoraka, 2013), as well know, but it is also more conservative with respect to other code-based approach (e.g. Turkish TBEC 2018, according to which a certain percentage of RC members can reach a given LS). Due to the main aim of this study, the sole distinction among the code cases applied herein lies in the implemented brittle capacity models, while the framework for determining the seismic capacity remains consistent with the European codes: the seismic demand is uniform across all code cases (in contrast to Dhanvijay and Nair, 2015), and the ductile capacity of beam/column elements is always defined as prescribed by EC8 2005 (and NTC 2018).

Within the codes framework, brittle failures are typically identified through post-processing the data obtained from (linear or) nonlinear analyses. However, it is worth noting that American standards also explicitly provide tools to model the nonlinear behaviour of shear-sensitive elements, including beam-column joints (i.e., scissor model, Alath and Kunnath 1995), providing the backbone for their implementation (ASCE/SEI-41, 2017; Hassan 2011; Hassan and Elmorsy 2022a,b).

Lastly, it is worth noting that, very recently, some works from the literature focused on the analysis of the capability of code prescriptions to catch real capacity and seismic damage extend and severity in existing buildings. Cook et al. (2023) and Sen et al. (2023) analysed the results of structures experimentally damaged via shake tables testing, to compare the experimental response with the simulated outcomes following ASCE/SEI 41 application, aiming at promoting its improvement. Similarly, in European context, a challenging work is currently ongoing by several European research groups to update the current European standards (e.g., Fardis (2021), Biskinis and Fardis (2020), Franchin and Noto (2023), Maranhão et al. (2024), among others). Therefore, a focus on the brittle capacity models of the (current draft of the) incoming second-generation Eurocode 8 - currently ongoing and in its final steps of development - is carried out in this work. Some studies from the literature have already started analysing the main differences compared to the current version. For instance, the design of moment resisting frame RC buildings according to the second-generation code has been compared to the previous EC8 version in Maranhão et al. (2024). The next-generation EC8 will modify the current shear strength model of beam-column joints (Fardis 2021) and change significantly the brittle capacity model to be used for beam/column members, moving from the empirical model by Biskinis et al. (2004) (EC8 2005) to a MCFT-based approach (Biskinis and Fardis 2020). Such novelties could potentially be very impactful and, thus, they are investigated in this work.

2 Overview of the current code-based shear capacity models worldwide

In this section, a description of some of the main shear capacity models currently adopted worldwide for beams/columns and joints is provided. The capacity models adopted by the current European (EC8 2005), Italian (NTC 2018; Circolare 2019), and American (ASCE/SEI) technical standards are analysed. A parametric comparison is also carried out to identify hierarchies and trends in resulting strengths.

2.1 Beams/columns shear strength models

Nowadays, worldwide, the shear strength of existing RC beam/column elements is generally evaluated using "degrading" models (De Luca and Verderame 2013), which predict a decreasing shear strength as the plastic displacement demand increases.

According to EC8 2005, the shear strength (V_R) of a beam/column element is calculated as proposed by Biskinis et al. 2004 ($V_{R,BIS}$), namely, as the sum of three contributions:

$$V_{R,EC8} = V_{R,BIS} = \frac{1}{\gamma_{el}}[V_N + k(V_c + V_w)] = \frac{1}{\gamma_{el}}\left[\frac{h-x}{2L_v}\min(N; 0.55A_c f_c) + k\left(\alpha\sqrt{f_c}A_c + \frac{A_{sw}f_{yw}}{s}z\right)\right] \quad (1)$$

In Eq. (1), the coefficient γ_{el}, accounting for uncertainties in fitting experimental data, is equal to 1.15 for primary elements. V_N is the contribution due to the presence of compressive axial load N (Paulay and Priestley 1992). The latter is limited to 55% of the maximum axial load that the concrete section can sustain (i.e., $A_c f_c$, being A_c the area of the concrete cross-section and f_c the concrete compression strength). h is the section height, x the neutral

axis depth, and L_V the element shear span. The contribution of the post-cracking concrete resistance mechanisms, V_c, can be expressed as α times $\sqrt{f_c} \cdot A_c$. The term α depends on the total geometric percentage of the longitudinal reinforcement, ρ_{tot}, and on the slenderness of the element, L_V/h. Lastly, the contribution of the transverse reinforcement, V_w, is the same proposed by Ritter-Morsch model (Ritter 1899; Morsch 1909). Thus, it depends on the stirrups area (A_{sw}), yielding strength (f_{yw}), and spacing (s), and on the internal lever arm (z) - assumed hereinafter as 0.9 times the cross-section effective depth, d.

According to EC8 2005, V_R degrades by means of the coefficient, k. The latter decreases as displacement ductility demand (μ_Δ) increases (Fig. 1), moving linearly from 1 (no degradation) to 0.75 (maximum degradation).

It is worth underlying that the EC8 2005 provides materials strengths reduction factors for safety check at SD LS. In particular, the mean strengths resulting from in-situ tests must be divided by the partial safety factor ($\gamma_c = 1.50$ for concrete and $\gamma_s = 1.15$ for steel) and by the Confidence Factor (i.e., CF) depending on the Knowledge Level (KL). In this work, a comprehensive KL has been always assumed, and, thus, CF = 1.00.

The same shear capacity model is (partially) adopted also by Italian technical code (NTC 2018), which introduces a modification for low μ_Δ levels, by using the truss model of shear resistance with variable inclination diagonals (Biskinis and Fardis 2004). The latter is hereinafter referred to as Variable Inclination Truss (i.e., VIT) model. In particular, V_R is the same provided by EC8 2005 model when $\mu_\Delta \geq 3$ (i.e., $V_{R,\,NTC18} = V_{R,\,EC8}$). When $\mu_\Delta \leq 2$, V_R is the maximum between the values provided by EC8 2005 model and VIT model. Lastly, for intermediate ductility demand, $V_{R,\,NTC18}$ is obtained by linearly interpolating between the two models (Fig. 1a). As well known, according to VIT model (prescribed for not-seismic loadings by NTC 2018 and EN 1998-1, 2004), the shear strength ($V_{R,VIT}$) is the minimum between compressed strut strength, V_{Rc}, and the tensile strength of the transverse reinforcement, V_{Rs}, i.e. (in case of stirrups):

$$V_{R,VIT} = \min(V_{Rc}; V_{Rs}) = \min\left(\alpha_c \bar{\nu} \; f_c \, b \, d \cdot \frac{1}{\tan\theta + \cot\theta}; \frac{A_{sw} f_{yw}}{s} 0.9d \cot\theta\right) \quad (2)$$

In Eq. (2), θ is the inclination angle of the compressed struts with respect to the longitudinal axis of the element, b the web width, $\bar{\nu}$ is equal to 0.5, and α_c is a function of N. According to Italian code, $\cot\theta$ in Eq. (2) mut be limited between 1.00 and 2.50.

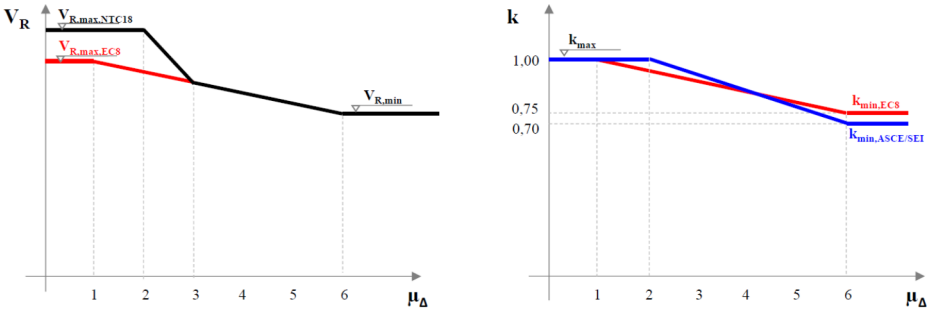

Fig. 1 Shear capacity model according EC8-2005 and NTC 2018 (**a**); degradation coefficient according to EC8 2005 and ASCE/SEI-41 (**b**)

Similarly to European code, Italian guidelines also require that materials strengths must be divided by the partial materials factors and by the CF for safety checks at SD LS.

The model adopted by ASCE/SEI ($V_{R,ASCE}$) is based on Sezen and Moehle (2004)'s model, i.e. an additive degrading model relying on two contributions: V_c, due to concrete post-cracking mechanisms and axial load, and V_w.

$$V_{R,ASCE} = k\,(V_c + V_w) = k\left[\left(\frac{0.5\sqrt{f_c}}{L_V/d}\sqrt{1+\frac{N}{0.5\sqrt{f_c}A_c}}\right)0.8A_c + V_w\right] \tag{3}$$

where V_w has the same meaning of Eq. (1). According to this model, the degradation coefficient k is equal to 1.00 for $\mu_\Delta \leq 2$, and 0.70 for $\mu_\Delta \geq 6$, varying linearly between these two bounds (Fig. 1b). ASCE/SEI model predicts a higher strength degradation compared to EC8 2005. Indeed, on one hand, the "residual" strength is derived from a lower degradation coefficient k ($k = 0.70$); on the other hand, this coefficient multiplies all the strength contributions (even that related to the axial load).

The material strengths to be used for assessment are, also in this case, the reduced strengths. However, while γ_c assumes the same value provided by European codes, γ_s is higher (i.e., 1.25). Furthermore, this standard prescribes that, in case of "comprehensive" knowledge (maximum level), CF is equal to the 1.

In existing structures, especially if designed for gravity loads only, structural elements often have low transverse reinforcement ratios. In this hypothesis, the strength provided by the VIT model, coincides with V_{Rs} evaluated with $\cot\theta = 2.5$. Thus, in these cases, $V_{R,VIT} = \min(V_{Rc}; V_{Rs}) = V_{Rs} = V_w \cot\theta = 2.5 V_w$.

For high plastic demands, Italian and European codes provide the same shear strength. On the contrary, a difference is observed when $\mu_\Delta \leq 3$. This difference (Eq. (4)) is maximized in absence of strength degradation ($k = 1$) and can be expressed as the sum of three terms. They depend on five parameters: axial load ratio $\nu = N/(A_c f_c)$, mechanical percentage of shear reinforcement $\omega_{sw} = A_{sw} f_y/(b \cdot s \cdot f_c)$, the above-defined L_V/h, ρ_{tot}, and the mean concrete compressive strength, f_{cm}.

$$\eta^{EC8-VIT} = \frac{\Delta V_R{}^{EC8-VIT}}{A_c f_{cm}} = \left(0.33\nu - 0.37\nu^2\right)\frac{1}{\frac{L_V}{h}} + \frac{11.40\rho_{tot}\left(1 - 0.16\frac{L_V}{h}\right)}{\sqrt{f_{cm}}} - 1.27\omega_{sw} \tag{4}$$

In Eq. (4), $\Delta V_R{}^{EC8-VIT}$ is the difference between $V_{R,EC8}$ and $V_{R,VIT}$, and it is normalized with respect to the quantity $A_c \cdot f_{cm}$. So, when the combination of the five parameters above leads to positive values of ΔV_R, $V_{R,EC8} > V_{R,VIT}$. Note that f_c and f_{cm} represent both the concrete compressive strength, but the latter is a mean value (derived from in-situ tests), whereas the former is evaluated as $f_c = f_{cm}/(CF \cdot \gamma_c)$.

The same normalized difference can be evaluated by comparing the non-degraded shear strengths resulting from the European and American codes, as shown in Eq. (5) (which results quite similar to Eq. (4)):

$$\eta^{\mathrm{EC8-ASCE}} = \frac{\Delta \mathrm{V_R}^{\mathrm{EC8-ASCE}}}{\mathrm{A_c f_{cm}}} = \left(0.33\nu - 0.37\nu^2 - 0.40\sqrt{\frac{0.67 + 1.09\nu\sqrt{\mathrm{f_{cm}}}}{\mathrm{f_{cm}}}}\right)\frac{1}{\frac{\mathrm{L_V}}{\mathrm{h}}} + \frac{11.40\rho_{\mathrm{tot}}\left(1 - 0.16\frac{\mathrm{L_V}}{\mathrm{h}}\right)}{\sqrt{\mathrm{f_{cm}}}} - 0.12\omega_{\mathrm{sw}} \tag{5}$$

Note that the expressions above assume that:

- ρ_{tot} is not lower than 0.50% (in tune with the definition of α in Eq. (1));
- ω_{sw} is compatible with the assumption of a weakly reinforced element (i.e., not exceeding 0.07, value which provides $\cot\theta$ always limited to 2.5), as typical in existing buildings;
- $\mathrm{L_V/h}$ ranges between 2 and 4 (considering the limitations of ASCE model);
- the cross-section height, h, has been confused with its effective depth, d, for sake of simplicity.

Figure 2 shows the isocurves corresponding to $\Delta \mathrm{V_R} = 0$ resulting from Eq. (4) (in grey scale) and Eq. (5) (in blue scale). They display when the code models provide the same strength. Three possible values of $\mathrm{L_V/h}$ and $\mathrm{f_{cm}}$ are assumed in Fig. 2 (i.e., $\mathrm{L_V/h} = 2; 3; 4$,

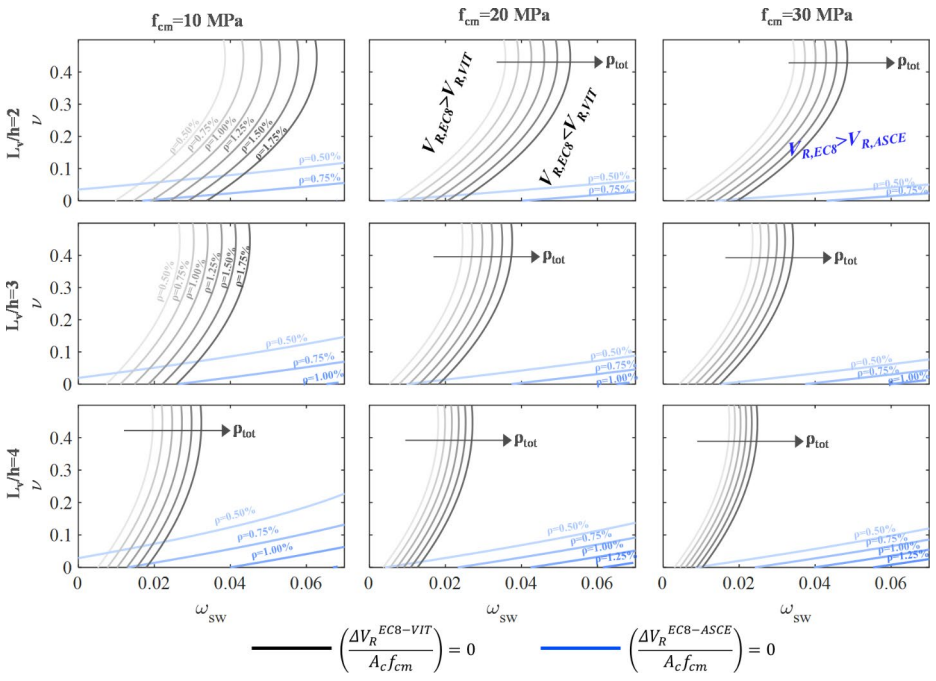

Fig. 2 Isocurves corresponding to $\Delta V_R = 0$, varying $\frac{L_V}{h}$, f_c, ω_{sw}, ν, and ρ_{tot}, resulting from the comparison between $V_{R,EC8}$ with $V_{R,VIT}$ (in gray scale) and with $V_{R,ASCE}$ (in blue scale)

and $f_{cm} = 10; 20; 30$MPa). The axial load ratio ν varies between 0 and 0.5. Each isocurve corresponds to a different value of ρ_{tot} (ranging between 0.50% and 2.00%). It can be noted that:

- for low values of ω_{sw} and high values of ν, $V_{R,EC8}$ results higher than the other two models. Actually, according to NTC 2018, for $V_{R,EC8} > V_{R,VIT}$, $V_{R,NTC18} = V_{R,EC8}$, and, thus, both codes provide exactly the same shear strength;
- the area where $\Delta V_R > 0$ covers wider ranges of ω_{sw} and ν values when ρ_{tot} is high;
- the latter effect is more pronounced when comparing $V_{R,EC8}$ and $V_{R,ASCE}$, and when considering upper bounds of f_{cm} and lower bounds of L_V/h.

Another useful representation of the differences among the considered models is shown in Fig. 3. A "central" value of $\eta^{EC8-VIT}$ (and $\eta^{EC8-ASCE}$) is calculated by using mean values (within the above-defined ranges of variation) of the 5 key parameters (central value of $\eta^{EC8-VIT}$ and $\eta^{EC8-ASCE}$ results −0.010 and 0.021, respectively). Then, the 5 parameters have been varied one-by-one to assume their upper or lower bound values (within the above-defined ranges of variation), and corresponding $\eta^{EC8-VIT}$ (and $\eta^{EC8-ASCE}$) are evaluated. Lastly, the relative variation (Ω) of $\eta^{EC8-VIT}$(and $\eta^{EC8-ASCE}$) with respect to the central value is plotted in Fig. 3a (and b). It is clear that ω_{sw} has the greatest influence on $\eta^{EC8-VIT}$, followed by ν, L_V/h and ρ_{tot}. The latter three parameters become more influent on $\eta^{EC8-ASCE}$, whereas f_{cm} always has a quite small importance in these comparisons (especially when comparing EC8 and ASCE).

A similar comparison can also be carried out focusing on the residual shear strength. The latter comparison makes sense only if $V_{R,EC8}$ and $V_{R,ASCE}$ are compared, since, when $\mu_\Delta \geq 3$, $V_{R,NTC18} = V_{R,EC8}$. By using the maximum degradation factors (i.e., k equal to 0.70 and 0.75 respectively for $V_{R,ASCE}$ and $V_{R,EC8}$), a small modification is observed in the coefficients of Eq. (5) (the values 0.40, 11.40, and 0.12 are replaced with 0.28, 8.52, and 0.05, respectively). The isocurves in Fig. 2 tend to shift towards lower ν and higher ω_{sw} values, making the area with positive ΔV_R much wider than that obtained for the non-degraded strength.

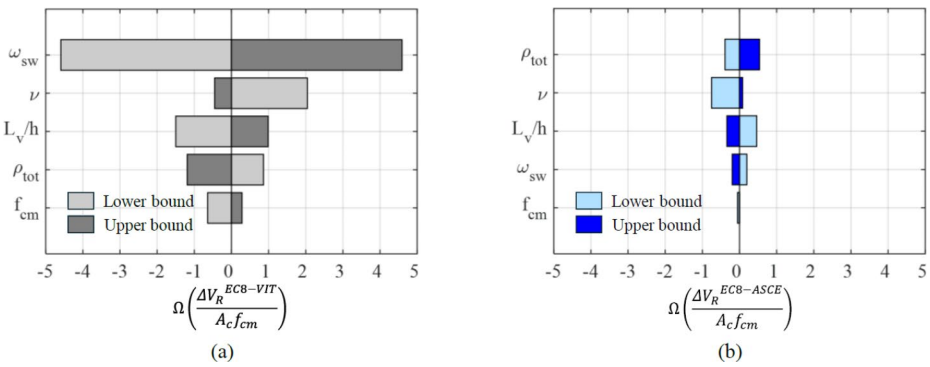

Fig. 3 Tornado diagrams for sensitivity analysis

2.2 Beam-column joints strength models

The capacity models of beam-column joints prescribed by current global standards differ to each other significantly both for reinforced (Del Vecchio et al. 2023) and unreinforced joints, especially when comparing the European approach with the American one.

According to EC8 2005, the shear strength of a beam-column joint is evaluated as in EN 1998-1, 2004, for newly designed buildings, by means of two safety checks (related to a tensile and a compressive failure mode). These checks can be reformulated in terms of joint shear stress $\tau_j = V_j/A_j$ (where V_j is the joint shear load and A_j the joint horizontal area, according to EN 1998-1, 2004) and normal vertical stress $\sigma_v = N/A_c$ (due to the axial force related to the column above the joint). By assuming a joint without stirrups (as typical in existing buildings), Eq. (6a) represents the tensile failure check, whereas Eq. (6b) the compressive failure check:

$$\tau_j \leqslant f_{ct}\sqrt{1+\frac{\sigma_v}{f_{ct}}} \tag{6a}$$

$$\tau_j \leqslant \eta f_c\sqrt{1-\frac{\sigma_v}{\eta f_c}} \tag{6b}$$

In Eq.s (6), η is equal to 0.60(1 - f_{ck}/250) for interior joints and 0.48(1 - f_{ck}/250) for exterior ones; f_{ct} is the concrete tensile strength (according to EN 1992-1-1, 2004). This strength, as well as the concrete compressive strength f_c, is intended to be the mean strength reduced by CF and partial materials safety factors (EC8 2005). Thus, $f_{ct} = f_{ctm}/(CF \cdot \gamma_c)$ with $f_{ctm} = 0.30\sqrt[3]{(f_{ck})^2}$). Conversely, f_{ck} is a characteristic concrete compression strength value, assumed equal to $(f_{cm} - 8)MPa$ (EN 1992-1-1, 2004).

For existing buildings, the Italian standard (Circolare 2019, C8.7.2.3.5) prescribes a double strength check for joints that are not fully confined according to Eq.s (6), as well. Nevertheless, it assumes $\eta = 0.50$ and $f_{ct} = 0.30\sqrt{f_c}$ (with $f_c = f_{cm}/(CF \cdot \gamma_c)$). As a results, comparing Italian and European codes, a difference in safety checks results is obtained even if both use Eq.s (6). Figure 4 shows this difference, distinguishing between exterior ("EXT J") and interior ("INT J") joints, and assuming three f_{cm} values to fix ideas.

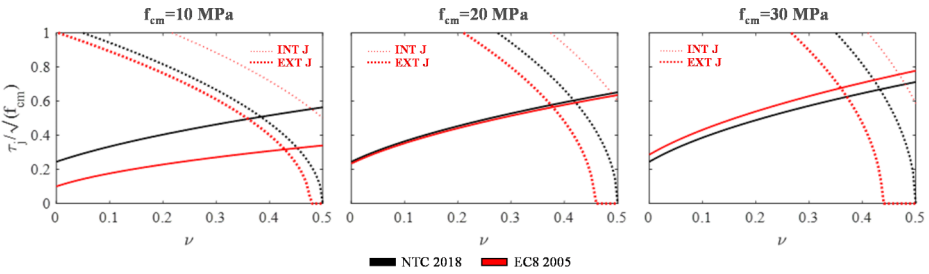

Fig. 4 Beam-column joint strengths according to EC8 2005 and NTC2018, given the joint configuration and the concrete compressive strength (tensile check with solid lines; compressive check with dotted lines)

For low values of f_{cm} (f_{cm} = 10 MPa), NTC 2018 model provides higher tensile joint strength (solid lines in Fig. 4) compared to EC8 2005; conversely, at higher values of f_{cm} (f_{cm} = 30 MPa), the hierarchy is reversed, with almost coincident strengths if f_{cm} = 20 MPa.

Regarding the compressive safety check (dotted lines in Fig. 4), EC8 2005 model provides a lower resistance in the case of exterior joints and a higher strength for interior ones.

However, for both European standards, the joint strength results as the minimum between those produced by Eq.s (6), given the value of ν. In other words, for low values of axial load ratio, the joint strength is limited by that corresponding to diagonal cracking (i.e. tensile failure), while for high ν, the joint fails due to compression failure.

According to American standard (ASCE/SEI), a joint shear stress capacity equal to $\lambda \gamma' \sqrt{f_c}$ is assumed, being λ = 1 for normal-weight aggregate concrete. The γ′ coefficient (see Table 1) depends on various parameters: joint typology (i.e., interior, exterior, or knee joint), presence/absence of transverse beams, presence/absence of "conforming" transverse reinforcement. Note that according to the American Code, if the stirrup spacing in the joint is less than or equal to half the column cross-section height, then the joint is considered as *conforming*. Otherwise, the joint is *nonconforming*. Thus, unlike EC8 2005 and NTC 2018, American standard prescribes a single safety check (Eq. (7)):

$$\tau_j \leq \gamma' \sqrt{f_c} \tag{7}$$

It should be noted that, while European standards lead to a joint strength variation with N, the American guideline always provides the same joint strength irrespective of the axial load level.

Another main difference of ASCE/SEI approach compared to European codes lies in the possibility of explicitly modelling the behaviour of the joint - possibility that could significantly impact the assessment outputs. This modelling is allowed by European standards as well, which, however, do not provide specific reference models.

In Fig. 5, the trend of the joint strength (expressed as $\tau_j/\sqrt{f_{cm}}$) is provided for fixed values of f_{cm}, depending on ν, according to all the strength models above.

For European models, the joint strength is evaluated for each axial load value as the minimum between tensile and compressive strength. This type of representation can be considered as a strength domain. Indeed, considering a given joint typology (i.e., interior or exterior) and a given f_{cm}, the demand joint shear load (i.e., V_j) and axial load (i.e., N) allow deriving the $\tau_j - \nu$ coordinates of a "demand point". If this point is inside or belongs to the boundary of the domain (related to the specific strength model), then the joint is on the safe side. The ascending branches of these domains represent the tensile check; the descending branches the compressive check.

Regarding American Code, joints are assumed as non-conforming herein, since, typically, stirrups in joints are totally missing in existing buildings. For interior joint (espe-

Table 1 Values of γ′ (= τ/√f_c) according to ASCE/SEI (in $MPa^{0.5}$)

Transverse reinforcements	Interior joints		Other joints		
	with transverse beams	Without transverse beams	With transverse beams	Without transverse beams	Knee joint
Nonconforming	1.00	0.83	0.67	0.50	0.33
Conforming	1.67	1.25	1.25	1.00	0.67

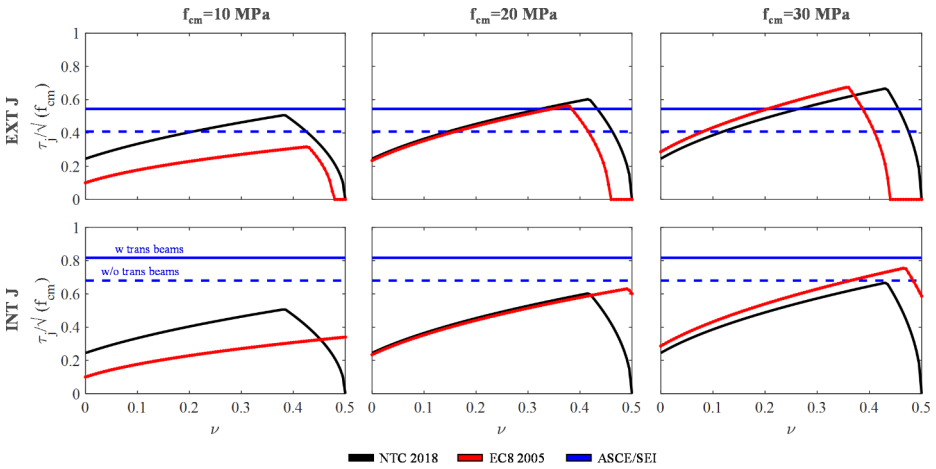

Fig. 5 Strength domains of beam-column joints according to NTC2018, EC8 2005 and ASCE/SEI, given the joint configuration and the concrete compressive strength

cially with transversal beams and low f_{cm} values), the joint strength is overestimated by ASCE/SEI compared with the European codes. Conversely, for exterior joints, the hierarchy among the models depends on ν and on f_{cm} values.

Moreover, ASCE/SEI provides a different strength for knee joints (i.e., $\gamma' = 4\ \sqrt{\text{MPa}}$). Being located on the top floor of the building, for these joints, zero axial load can be assumed. Thus, the joint strength according to European models can be obtained assuming $\sigma_v = 0$ in Eq.s (6) (i.e., ν=0 in Fig. 5), generally resulting lower than joint strength by ASCE/SEI.

3 Shear capacity models according to the next-generation of Eurocodes

In the previous section, the capacity models prescribed by current standards have been analysed and compared. However, a paramount work is currently ongoing by European research groups to update the current European standards with a second-generation of Eurocodes in the next years. Significant changes will be carried out to the shear strength models of both beam/column elements and beam-column joints, as highlighted by the recently published works from the literature (Biskinis and Fardis 2020; Fardis 2021; Franchin and Noto 2023). Thus, in this section, the capacity models introduced by the incoming second-generation of Eurocodes will be first analysed, emphasizing their evolution with respect to the current version. The current available drafts of the second-generation of Eurocodes adopted herein are prEN 1998-3:2023, FprEN 1998-1-1:2024 (along with its previous draft FprEN 1998-1-1:2022), and FprEN 1992-1-1:2023, along with the relevant references from the literature, recalled in the next sub-paragraphs.

3.1 Beams/columns shear strength

In the second-generation of Eurocode 8-part 3 (prEN 1998-3:2023), the shear capacity of existing RC beams and columns must be evaluated according to a model based on the variable inclination, θ, between the compression stress field in the member web and the member axis (Biskinis and Fardis 2020).

PrEN 1998-3:2023 prescribes to evaluate the shear strength, $V_{R,EC8-2nd}$, according to FprEN 1998-1-1:2024, by using the mean values of the material properties and also following FprEN 1992-1-1:2023 suggestions, even if with some modifications explained below. $V_{R,EC8-2nd}$ can be expressed as in Eq. (8):

$$V_{R,EC8-2nd} = \min\left(\frac{A_{sw}f_{yw}}{s}0.9d\cot\theta\ ;0.5\ \bar{\nu}\ \ f_c b_w 0.9\,d\right) + V_N \tag{8}$$

In Eq. (8), V_N is evaluated similarly to Eq. (1), and the variable inclination θ has the same meaning of the VIT model, ranging between 1 and $\cot\theta_{\min}$ (see Eq. (9)). The latter depends on the axial load, N.

$$\cot\theta_{\min} \geq \cot\theta = \sqrt{\frac{\bar{\nu}}{\omega_{sw}} - 1} \geq 1 \tag{9}$$

However, $\cot\theta$ may exceed the upper limit, $\cot\theta_{\min}$, if the deformation state of the cross-section is analysed. In fact, the value of $\bar{\nu}$ is not necessarily a constant value (i.e., 0.5 as prescribed by the VIT model), and it can be obtained based on the state of strains of the member according to Eq. (10) (FprEN 1998-1-1:2024):

$$\bar{\nu} = \frac{1}{1.6}\left(\frac{1}{1 + 110\,(\epsilon_x + (\epsilon_x + 0.001)\cot^2\theta)}\right) \leq 1 \tag{10}$$

where the reduction factor 1/1.6 is applied to account for cycling loading (Biskinis and Fardis 2020), and ϵ_x is the average strain between the bottom and top chords, ranging between 0 and 0.02 (FprEN 1998-1-1:2024). Note that, strictly speaking, according to FprEN 1998-1-1:2024 draft, $\bar{\nu}$ in seismic loading conditions should be always higher than 0.5/1.6 (=0.31). However, the latter prescription was not present in the previous draft (FprEN 1998-1-1:2022), nor in original works by Biskinis and Fardis (2020); additionally, it would result very close to the TIV model and in a not safe-sided prescription. Thus, it has not been applied in what follows.

ϵ_x is calculated as in Eq. (11) (FprEN 1992-1-1:2023):

$$\epsilon_x = \frac{\epsilon_{xt} + \epsilon_{xc}}{2} = \begin{cases} 0.5\left[\left(\frac{F_{td}}{A_{st}E_s}\right) + \left(\frac{-F_{cd}}{A_{cc}E_c}\right)\right] & if\ the\ flexural\ compression\ chord\ is\ in\ compression \\ 0.5\left[\left(\frac{F_{td}}{A_{st}E_s}\right) + \left(\frac{|F_{cd}|}{A_{sc}E_s}\right)\right] & if\ the\ flexural\ compression\ chord\ is\ in\ tension \end{cases} \tag{11}$$

where A_{st} and A_{sc} are the areas of the longitudinal reinforcement in the flexural tension chord and flexural compression chord, respectively; A_{cc} is the area of the flexural compres-

sion chord. Lastly the "chord forces", F_{td} and F_{cd}, are defined as a function of the flexural (M_{Ed}) and shear (V_{Ed}) demand, and of axial force.

$$\begin{cases} F_{td} = \frac{\mu_\Delta M_{Ed}}{z} + \frac{\mu_\Delta V_{Ed}\cot\theta + N}{2} \\ F_{cd} = \frac{\mu_\Delta M_{Ed}}{z} - \frac{\mu_\Delta V_{Ed}\cot\theta + N}{2} \end{cases} \tag{12}$$

Moreover, in member end-zones expected to enter the inelastic range, the values of M_{Ed} and V_{Ed} from the analysis should be multiplied by the chord rotation ductility factor, μ_Δ. It is worth noting that the approach proposed in Eq. (12) is a simplified approach, based on the assumption of the equal displacement rule. Nevertheless, the effective average strain ϵ_x should be rigorously evaluated, considering the curvature and the neutral axis depth of the cross-section (Biskinis and Fardis 2020).

The additional tensile axial load, $V_{Ed}\cot\theta$, and factor $\bar{\nu}$ depend on $\cot\theta$, resulting in an iterative procedure to derive the inclination θ and, thus, the shear capacity $V_{R,EC8-2nd}$.

Lastly, in the code-based safety check at SD LS, the shear resistance of existing members (prEN 1998-3:2023), should be divided by the corresponding safety factor related to the resistance, γ_{Rd} (prEN 1998-3:2023). The latter accounts for uncertainty in the shear strength assessment and is evaluated as in Eq. (13) (Franchin and Noto 2023):

$$\gamma_{Rd} = \exp\left(\alpha_R \beta_{LS,CC} \sigma_{lnR}\right) \tag{13}$$

In Eq. (13), α_R is the resistance sensitivity factor, equal to 0.85 according to FprEN 1998-1-1:2024 and Franchin and Noto (2023). The target reliability index in a 50-years reference period, $\beta_{LS,CC}$, depends on both the considered limit state and the consequence class. According to the Annex F of FprEN 1998-1-1:2024, for SD LS and CC2 (second consequence class), $\beta_{LS,CC}$ is equal to 1.60. Lasty, the total logarithmic standard deviation σ_{lnR} for existing members with rectangular cross-section is equal to 0.40 (prEN 1998-3:2023-Table 8.5) when the KL3 is attained, as assumed herein. As a result, $\gamma_{Rd} = 1.72$ is obtained herein.

3.2 Beam-column joints

According to PrEN 1998-3:2023, the shear resistance of existing beam-column joints should be evaluated as prescribed for new elements (prEN 1998-1-1:2024). Based on prEN 1998-1-1:2024, for unreinforced joints a cracking strength ($V_{Rj,cr}$) only is provided. Vice-versa, in presence of transverse reinforcement, $V_{Rj,cr}$ can be overcome and joint strength estimated based on studies by Fardis (2021). Nevertheless, prEN 1998-1-1:2024 also specifies that, in a safe-side and simplified approach, joint strength can be calculated as the maximum between the shear resistance at the first cracking and a minimum value of joint strength ($V_{Rj,min}$), the latter related to the absence of transverse reinforcement and axial load:

$$V_{j,EC8-2nd} = \min(V_{Rj,cr}; V_{Rj,min}) = \min\left(f_{ctm}\sqrt{1 + \frac{N}{A_c f_{ctm}}}A_j; \alpha f_{ctm} b_j \sqrt{h_c h_b}\right) \tag{14}$$

In Eq. (14), α is equal to 0.5 for exterior joints and 1.2 for interior ones, h_b and h_c are the beam and column depth, respectively, and other parameters have been defined above. Eq. (14) is applied herein to calculate the shear strength of unreinforced joints according to the second-generation Eurocode. Thus, a first comparison with EC8 2005 can be easily carried out, as shown in Fig. 6, in terms of shear stress $\tau_j/\sqrt{f_{cm}}$, and, assuming four h_b/h_c ratios (i.e., 500 mm/[300 400 500 600]mm). It is worth noting that, ν in Fig. 6 is defined as a function of f_{cm}, both for EC8 2005 (contrary to what Fig. 5 shows) and for the incoming-code, for sake of comparison. Additionally, the application of γ_{Rd} factor for joints is not foreseen in the currently available drafts (i.e., γ_{Rd}=1). However, it is reasonably very likely that in the final version of Eurocode 8, a γ_{Rd} factor similar to those used to reduce the shear strength of beams/columns will be introduced. For this reason, herein, the joint strength has been assessed with a twofold assumption: γ_{Rd}=1 and γ_{Rd}=1.72.

Unlike EC8 2005, the current draft of the second-generation Eurocode does not explicitly provide a compression limitation for unreinforced joints, leading to a different shear strength-axial load trend for high axial load ratios (even for ν<0.3 for exterior joints). Instead, the presence of a minimum strength leads to higher $V_{j,\,EC8-2nd}$ in the case of interior joint, especially for low axial loads and high values of the h_b/h_c. Therefore, moving from the first to the second generation, a lower number of joint failures can be expected for the top floors interior joints (if characterized by lower h_c values, i.e., higher h_b/h_c ratios and lower axial loads). Moreover, the use of a γ_{Rd} coefficient higher than 1 significantly reduces the joint strength, and, consequently, its hierarchy with respect to the current Eurocode (see Fig. 6).

4 Case-study buildings: description and modelling

According to the ISTAT (2011) census, roughly 1/3 of Italian RC buildings have been built before 1970, when most of the national territory (about 6700 municipalities) was classified as not-seismic prone area. About 2% of municipalities not seismically classified before

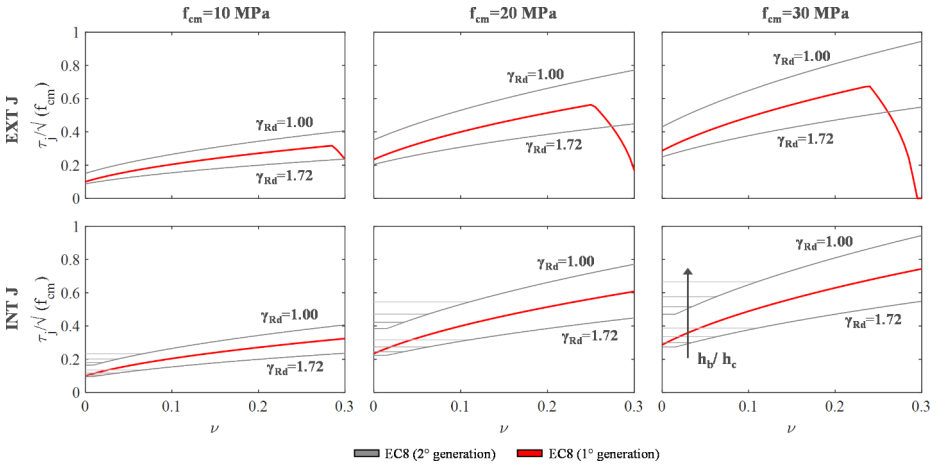

Fig. 6 Strength domain for unreinforced beam-column joints: comparison between first- and second-generation of Eurocodes

1970 are nowadays classified as first seismic zone, based on expected value of acceleration on stiff soil (a_g) with 10% probability of exceedance in 50 years exceeding 0.25 g. 23% is classified as second seismic zone ($0.15 < a_g \leq 0.25$ g), about the 60% as third ($0.05 < a_g \leq 0.15$ g) and the 17% as fourth ($a_g \leq 0.05$ g) seismic zone.

In this section, two case-study buildings have been selected to analyse the difference among code-based brittle capacity models described in Sects. 2 and 3. They are RC residential buildings designed according to the technical regulations in force in Italy until 1970 (Royal Decree, R.D. 2229, 1939), to withstand only gravity loads, located in the about 6700 municipalities mentioned above. Case-study buildings haves the same floor area, but different number of stories, Ns (2 and 4), being buildings with $Ns \leq 4$ the most widespread in Italian building stock (ISTAT 2011).

4.1 Buildings description

The selected case study buildings are in line with the prevalent construction practices in force in Italy before '70s. Each structure has a Moment Resisting Frame (MRF) system, consisting of 2D parallel resisting frames in the longitudinal (X) direction (see Fig. 7a), without interior beams in the transverse (Y) direction. Buildings are symmetric in both directions (X and Y). Floor slabs are 20 cm width, and the inter-story height is 3.00 m (see Fig. 7b).

The cross-section dimensions and reinforcement details are based on a simulated design (Verderame et al. 2010; De Risi et al. 2023b) according to the Italian code in force during the construction period (R.D.2229, 1939). A maximum allowable stress of 5.0 or 6.0 MPa was considered for concrete (depending on compressive loads or bending actions, respectively), and of 140 MPa for reinforcing plain bars (type AQ42). All the beams have a 30×50 cm² cross-section, with a geometrical percentage of longitudinal reinforcement (ρ_l) ranging from 0.40% to about 0.90%– see Fig. 7c. Column sections (Fig. 7d) vary from 30×30 cm² (for the upper storeys) to 30×40 cm² (for the central columns of the ground floor of the 4-storey building), with a decreasing reinforcement ratio from the ground floor of the 4-storey building ($\rho_l \approx 0.80\%$) to the last floor ($\rho_l \approx 0.60\%$). The minimum requirement specified by the R.D.2229 (1939) is adopted as transverse reinforcement (Fig. 7c, d). Note that no transverse reinforcement was placed within beam-column joints, since the technical code in force at the construction time did not require any design nor reinforcement of joints. Additional information about the main buildings features is reported in De Risi et al. (2023a).

Lastly, f_{cm} and mean yielding strength of rebars (f_{ym}) used for buildings assessment are assumed equal to 20 MPa and 322 MPa, respectively, according to Verderame et al. (2010) and Masi et al. (2019), for the relevant time period.

Resulting first mode periods (T_X and T_Y), mass participation ratios ($m_{p,x}$ and $m_{p,y}$) in both the main directions, and the seismic weight (W), ranging between 8.6 and 10 kN/m², are also shown in Table 2.

4.2 Modelling assumptions

Each building is modelled in the OpenSees platform (McKenna 2011) with 3D "bare" frames. Beams and columns are modelled as ductile elements using a lumped plasticity approach to simulate their flexural response (see Fig. 8). This approach is implemented

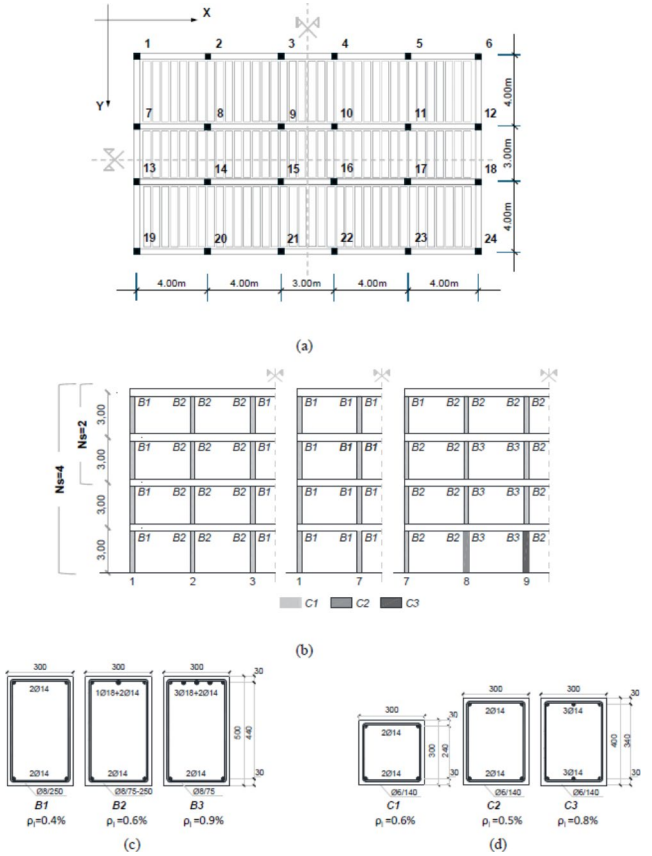

Fig. 7 Plan view (**a**) of case-study buildings and related representative frames (**b**); cross-sections of typical beams (**c**) and columns (**d**) (dimensions in millimetres)

Table 2 Modal properties of the case-study buildings

Ns	W (ton)	T_X (s)	T_Y (s)	$m_{p,x}$ (%)	$m_{p,y}$ (%)
2	404	0.37	0.51	93	86
4	852	0.71	1.04	87	83

by elastic *BeamColumn Elements* in series with *Zero-Length Elements* (featuring by the *Pinching4 Uniaxial Material*) at both ends of each beam/column. The flexural response is a moment (M)-chord rotation (θ) relationship calibrated for RC elements reinforced with plain bars (Verderame and Ricci 2018), by means of a four-point envelope, integrated herein by an additional point corresponding to the first cracking (Fig. 8).

Masonry infills are only considered in terms of masses and loads. It is acknowledged that masonry infills play a crucial role on seismic performance of RC buildings. Nevertheless, despite decades of research about this topic, often codes worldwide do not provide comprehensive provisions for numerical modelling of masonry infills and relevant safety checks. This is the case of Italian code (D.M. 2018), and of the current European code (CEN, 2004) as well. As an example, no information about the in-plane nonlinear response, or, more

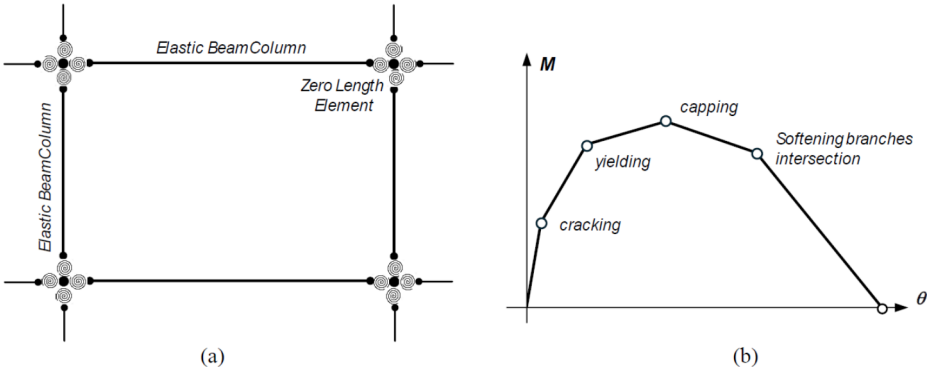

Fig. 8 Adopted lumped plasticity approach (**a**); envelope of the flexural response of beams and columns (**b**)

simply, the elastic stiffness of the infill panels is provided within these codes. Additionally, even the evaluation of infills mechanical properties (e.g., Young modulus or compressive strength) in existing buildings is still a challenging issue in common practice. As a result, in common practice, both for the design of new buildings and the assessment/retrofit of existing ones, infills are neglected (except than as loads and masses). Since this work is intended to be a code-based study, masonry infills are not explicitly modelled. Nevertheless, it is worth noting that a comprehensive risk-based analysis should certainly consider explicitly the presence of infills, if the main aim is a more "realistic" assessment of seismic performance and its improvement, along with a realistic estimation of seismic losses (De Risi et al. 2020a; Del Gaudio et al. 2021).

Similarly, following a typical practice-oriented approach, joints are assumed to be rigid elements, and the floors stiff in their own plane. Lastly, potential shear failures have been identified in post-processing, considering all models introduced in Sects. 2 and 3.

5 Seismic capacity of case-study buildings at SD LS

The code-based assessment at a given LS can be expressed through a capacity-to-demand ratio. NTC 2018 allows to synthetically express this ratio in terms of Peak Ground Acceleration (PGA). The demand mainly depends on the considered LS and the construction location and use. The capacity depends on the attainment of a certain failure condition, generally the first failure occurring at the considered LS (NTC 2018, EC8 2005). The adopted capacity model certainly affects the capacity. This is particularly true for the shear strength models, since brittle failures generally limit the seismic capacity of existing buildings (De Risi et al. 2023a).

Therefore, in this section, the first achievement and the evolution of brittle failures at SD LS is illustrated, depending on the adopted shear capacity models. Then, the influence of the capacity models on the buildings seismic assessment is analysed, assuming as possible buildings locations all Italian municipalities classified as seismic-prone only after 1970.

5.1 SPO curves and failure mapping

The seismic capacity assessment is performed within the N2 framework (Fajfar 2000). Non-linear static pushover analyses are carried out, considering a lateral load distribution proportional to the first vibration modal shape in each direction. The resulting capacity curves (obtained as suggested by European codes, NTC 2018 and EC8 2005), are shown in Fig. 9, as spectral displacement (S_d) -versus- pseudo-acceleration (S_a(T) up to the occurrence of the first ductile failure (DF) at the SD LS. As suggested by the Italian code, such failure occurs when the demand in terms of chord rotation θ reaches ¾ of the capacity calculated according to Biskinis and Fardis (2010). Since the focus of the present work is on brittle failures models, such definition of DF capacity point is always kept constant in what follows.

In addition to the capacity curves, also the relevant collapse mechanisms are shown in Fig. 9. A global collapse mechanism is always observed in the transverse (Y) direction, whereas local mechanisms are observed in the longitudinal (X) direction. Each capacity curve also shows the achievement of all the failure typologies at SD LS, i.e. the first joint failure (JF), and the first shear failure (SF) in beams or columns, according to the considered capacity models. Moreover, the percentage of failing elements is provided in each step of the pushover analysis.

Regarding the beams/columns SFs (which occur only in the X direction on the lowest storeys of the case-study buildings), the most conservative capacity model for the analysed case-study buildings is that proposed by EC8 2005. Only according to this model, even the 2-story building exhibits SFs (especially in the longitudinal exterior beams at the first floor). Considering the other two codes, ASCE/SEI results the less conservative model.

About beam-column joints, current European technical regulations (NTC 2018, EC8 2005) prescribe a dual check. The tensile failure is hereinafter referred to as JF(T). The compression failure is labelled JF(C). It is worth noting that a joint does not necessarily reaches its maximum capacity when diagonal cracking first occurs (Hakuto et al. 2000). In these cases, the occurrence of JF(T) could severely limit the actual joint capacity.

Considering JF(T) according to NTC 2018, failures occur in both directions for all the case studies, with a maximum percentage of failing elements in X direction that exceeds 50% of all the joints. The number of failures is about the same moving from the NTC 2018 to EC8 2005 model. Indeed, the diagonal tensile check according to NTC 2018 and EC8 2005 provides very similar capacity when f_{cm} = 20 MPa (Fig. 5).

On the contrary, JF(C), which represent a more appropriate failure criterion (Hakuto et al. 2000; Park and Mosalam 2012; NZS 3101, 2006), involves fewer joints (always below 10% of all the joints) of the tallest building, according to NTC 2018 and EC8 2005 models. The joints exhibiting JF(C) are typically interior joints with high axial loads. For this type of joints, EC8 2005 provides higher capacity than NTC 2018 (Fig. 5), thus delaying the first JF(C) (of the interior 8-11-14-17 joints at the first floor– see numeration in Fig. 7a).

Only one safety check is performed according to the American code for joints. Its relevant failure evolution is plotted in Fig. 5 with JF(T) of European codes, since that generally limits the building capacity. ASCE/SEI results less conservative than European codes (see Fig. 5), especially for interior joints.

The seismic capacity assessment at the SD LS is, lastly, carried out according the next-generation Eurocodes, assuming a double option for γ_{Rd} (1 or 1.72), as explained above.

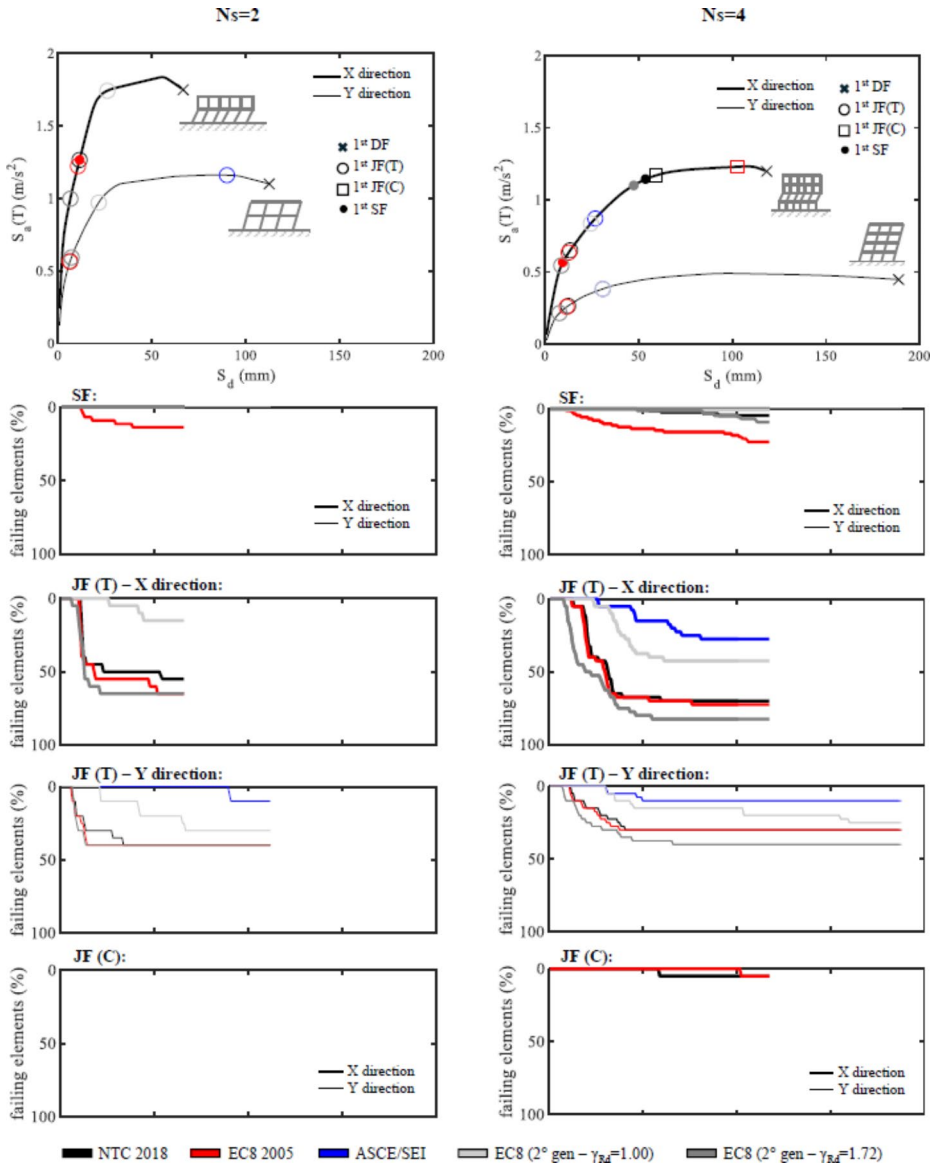

Fig. 9 Capacity curves up to the first DF with the relevant collapse mechanisms; evolution of the brittle failures at SD LS according to all considered code-based capacity models

With respect to the current EC8, the shear strength model by the second-generation Eurocodes leads to a lower number of SFs in beams/columns, even by using γ_{Rd}=1.72. Such failures primarily involve the internal longitudinal beams of the central spans and the central columns (i.e., 8-10-14-16) on the ground floor of the 4-storey building. Note that, if γ_{Rd}=1 was used, shear failures in beams/columns are not observed at all.

About JFs(T), the current European model provides intermediate results compared to those of the future Eurocode 8 considering the two γ_{Rd} bounds (coherently with Fig. 6). However, for the 2-story building, the number of JFs(T) is approximately the same when applying the strength model of the current Eurocode or that of the second generation with γ_{Rd}=1.72. As the number of stories increases, the maximum axial load increases at the bottom stories, and, thus, the unreinforced joint strength from the second-generation Eurocode tends to coincide with that related to cracking, leading to an increase in JF(T) failures even for interior joints (with γ_{Rd}=1.72) (see Fig. 6). If γ_{Rd}=1, a lower number of joint failures is always obtained with respect to the current Eurocode 8.

5.1.1 Influence of joints modelling on the buildings assessment

As clearly highlighted above, the shear failure of joints can significantly limit the building seismic capacity. It is worth noting that the safety check of beam-column joints is often very penalizing because of the use of a force-based approach (i.e., a comparison between shear load and shear strength), in conjunction with the definition of LS achievement when the first element fails. A possible alternative is offered, among the investigated codes, by ASCE/SEI guidelines. ASCE/SEI explicitly introduces the possibility to model the nonlinear response of beam-column joints, for example using the so-called scissors model, shown in Fig. 10(a) (ASCE/SEI 41, 2017; Alath and Kunnath 1995). ASCE/SEI also explicitly provides the characterization of the joint nonlinear response and the joint shear strain (γ_j) thresholds to be used for each LS safety check, thus actually introducing the possibility of a displacement-based approach also for elements like joints.

Both the strain thresholds and the whole joint nonlinear response depend on the joint typology, the axial load ratio, the shear load level, and the presence of (conforming or not) stirrups. A typical nonlinear response of the beam-column joints according to ASCE/SEI suggestion is reproduced in Fig. 10(b) (ASCE/SEI 41, 2017; Hassan 2011). These prescriptions by American guidelines have been applied to the buildings analysed herein for a brief comment, in this sub-section only, about the influence of joint modelling, by:

- implementing the scissors model (Alath and Kunnath 1995) as in Fig. 10(a);
- converting the joint shear stress into joint moment (M_j) as suggested in the literature based on equilibrium equations (Celik and Ellingwood 2008; De Risi et al. 2017); and.
- assuming that the joint rotational spring is equal to γ_j (Celik and Ellingwood 2008; De

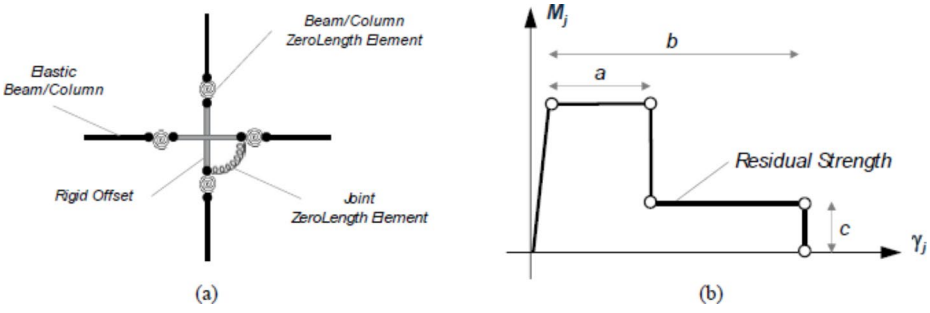

Fig. 10 Scissors model for beam-column joints (**a**); nonlinear response of the beam-column joint according to ASCE/SEI (**b**)

Risi et al. 2017).

The joint spring is characterized based on f_{cm} as concrete compressive strength, without any reduction coefficient. The achievement of SD LS is (conservatively) assumed herein as the attainment of the beginning of the joint softening response (i.e., when the second point of Fig. 10(b) is reached for the first time in a joint spring). Pushover curves are updated following this modelling approach.

As a result, for the analysed 2- and 4-storey buildings, joint failures are not detected at all, thus highlighting the great difference in safety check depending on the check approach.

5.2 Seismic capacity

For each building and direction, the capacity curve is bi-linearized according to NTC 2018, obtaining an elastic-perfectly-plastic curve. Since the focus of the present work is on brittle failures models, the bi-linearization approach is kept always constant in what follows.

Starting from the inelastic capacity point, C_{IN} (i.e., the attainment of the first failure at the SD LS on the elasto-plastic bilinear curve), the corresponding elastic capacity point, C_{EL}, is derived by means of Vidic et al. (1994) relationships. Vidic et al. (1994) proposal depends on the ratio between the building effective period, T_{eff}, and the corner period T_C. The latter is a function of the building location according to NTC 2018, always used herein to characterize seismic hazard. Considering the demand elastic spectra at the SD LS (with return period 475 years) for all the considered sites– always assuming soil type A (NTC 2018, EC8 2005)–, the equal-displacement condition always applies herein (being $T_{eff,\,X}$=0.55s and $T_{eff,\,Y}$=0.99s for Ns=2, and $T_{eff,\,X}$=0.77s and $T_{eff,\,Y}$=1.46s for Ns=4). The elastic spectral pseudo-acceleration capacity, $S_{a,C}(T_{eff})$, is shown in Fig. 11 for each building/direction/code.

In almost all buildings/codes, the very first failure occurs on the linear branch of the bilinear capacity curve (resulting in C_{EL}=C_{IN}). The exceptions are the first failures in the Y direction for all buildings, and in the X direction for the 2-story building, according to ASCE/SEI and next generation EC8 wth γ_{Rd}=1. Note that in these cases, the values of $S_{a,\,C}(T_{eff})$ were cut off from the plot, being very high (see Table 3). In general, the $S_{a,\,C}(T_{eff})$ evaluated according to American standards is significantly higher compared to those obtained with (current or incoming) European models. Instead, the values provided by Italian and European standards are quite similar to each other, especially in Y direction (see Table 3).

The pseudo-acceleration spectrum passing through the elastic capacity point C_{EL} allows associating a capacity PGA value (PGA_C) to each site (as described in De Risi et al. 2023a). An example is shown in Fig. 12a. Given C_{EL} point and the spectral parameters of each site

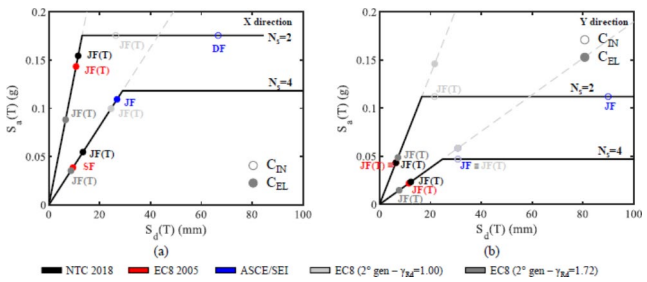

Fig. 11 As-built capacity in terms of $S_a(T_{eff})$ at SD LS: X-(**a**) and Y-(**b**) direction

Table 3 Capacity in terms of $S_a(T_{eff})$ and PGA in both direction assuming A-soil type (expressed in g)

N_S		2		4	
Direction		X	Y	X	Y
NTC 2018	$S_{a,C}(T_{eff})$	0.154	0.043	0.055	0.023
	$PGA_{C,16}$	0.086	0.043	0.059	0.043
	$PGA_{C,50}$	0.104	0.049	0.072	0.050
	$PGA_{C,84}$	0.123	0.054	0.082	0.055
EC8 2005	$S_{a,C}(T_{eff})$	0.143	0.043	0.039	0.022
	$PGA_{C,16}$	0.080	0.043	0.047	0.042
	$PGA_{C,50}$	0.098	0.049	0.055	0.047
	$PGA_{C,84}$	0.115	0.054	0.060	0.052
ASCE/SEI	$S_{a,C}(T_{eff})$	0.893	0.605	0.109	0.058
	$PGA_{C,16}$	0.421	0.403	0.104	0.086
	$PGA_{C,50}$	0.546	0.523	0.131	0.105
	$PGA_{C,84}$	0.659	0.63	0.154	0.124
EC8 (2nd gen– $\gamma_{Rd}=1.00$)	$S_{a,C}(T_{eff})$	0.353	0.146	0.100	0.058
	$PGA_{C,16}$	0.171	0.107	0.097	0.086
	$PGA_{C,50}$	0.223	0.136	0.120	0.105
	$PGA_{C,84}$	0.261	0.159	0.142	0.124
EC8 (2nd gen– $\gamma_{Rd}=1.72$)	$S_{a,C}(T_{eff})$	0.088	0.049	0.035	0.015
	$PGA_{C,16}$	0.054	0.046	0.044	0.032
	$PGA_{C,50}$	0.065	0.054	0.051	0.034
	$PGA_{C,84}$	0.074	0.060	0.056	0.038

at SD LS (according to NTC 2018), as many spectra passing through C_{EL} as the considered sites can be derived. Each of these spectra is characterised by a PGA_C value. Thus, PGA_C exhibits a certain variability, which clearly stems from the variability of the spectral shape associated with the building location (NTC 2018). Table 3 provides the median values and the 16th and 84th percentiles of PGA_C values ($PGA_{C,50}$, $PGA_{C,16}$, and $PGA_{C,84}$, respectively) for both directions. The minimum value of PGA_C is always in Y direction.

In Fig. 12b, the PGA_C (hereinafter, the minimum value between the two directions) is provided, showing median values, 16th and 84th percentiles. The capacity values according to EC8 2005, NTC 2018 and next-generation Eurocode derive from the same kind of failure (i.e., JF(T) in Y direction). According to the ASCE/SEI code, too, the capacity at the SD LS is due to a JF, which nevertheless generally occurs for higher displacement demands (see Fig. 9), resulting in higher PGA_C values (especially for Ns = 2). The coefficients of variation (CoV) of PGA_C are quite small (about 18% for both case studies in accordance with ASCE/SEI and next-generation EC8 with $\boldsymbol{\gamma_{Rd}}=1$; about 10% for the other cases).

Lastly, Fig. 12c shows the PGA_C ratios between the value corresponding to flexible soil types - from B to D (NTC 2018) - and that related to soil A (Fig. 12b), assumed as a reference. Moving from a rock soil (type A) to a more deformable soil (type D), PGA_C progressively decreases for all codes, up to about 50%.

Lastly, the as-built assessment explained above has been repeated by changing f_{cm}, assuming 10 MPa and 30 MPa, as in Sects. 2–3. Table 4 summarizes the results of this further analysis in terms of variation of $PGA_{C,50}$ (soil A) with respect to the results presented above (for f_{cm}=20 MPa), namely in terms of $\Phi PGA_{C,50}$= $PGA_{C,50,fcm}$ /$PGA_{C,50,fcm=20MPa}$. A lower value of f_{cm} leads to lower PGA_C (and more brittle failures); vice-versa if f_{cm}

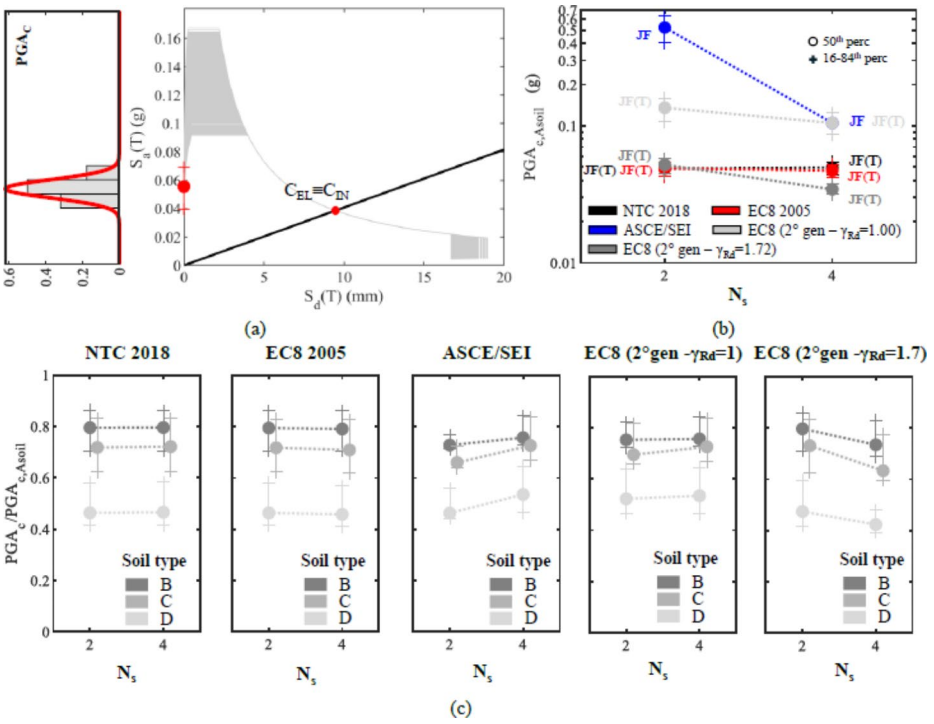

Fig. 12 Example of PGA_C derivation (4-storey building in X direction, according to EC8 2005 code) (**a**); PGA_C depending on Ns and code, assuming A soil type (**b**) and varying the soil typology (**c**)

Table 4 $\Phi PGA_{C,50}$ varying f_{cm} with respect to f_{cm}=20 MPa; relevant first failure typology in italic (bold text represents variation in the first failure with respect to the case f_{cm}=20 MPa)

$\Phi PGA_{C,50}$	f_{cm} = 10 MPa				f_{cm} = 30 MPa			
N_S	2		4		2		4	
Direction	X	Y	X	Y	X	Y	X	Y
NTC 2018	0.67	0.79	0.00	0.00	1.27	1.21	1.10	1.15
	JF(T)	JF(T)	**JF(C)**	**JF(C)**	JF(T)	JF(T)	JF(T)	JF(T)
EC8 2005	0.00	0.00	0.00	0.00	1.50	1.53	1.36	1.68
	JF(T)	JF(T)	**JF(T)**	JF(T)	**SF**	JF(T)	SF	JF(T)
ASCE/SEI	0.34	0.23	0.66	0.69	1.22	1.52	1.38	1.28
	JF	JF	JF	JF	DF	**DF**	JF	JF
EC8 (2° gen– γ_{Rd} = 1.00)	0.12	0.19	0.25	0.23	2.98	5.88	1.67	6.91
	JF(T)	JF(T)	JF(T)	JF(T)	**DF**	**DF**	JF(T)	**DF**
EC8 (2° gen– γ_{Rd} = 1.72)	0.00	0.00	0.00	0.00	2.25	1.68	1.24	1.91
	JF(T)	JF(T)	JF(T)	JF(T)	JF(T)	JF(T)	JF(T)	JF(T)

increases. Nevertheless, such a variation has different weight depending on the considered building and, above all code. For the 2-storey building:

- according to NTC 2018, the considered variation in f_{cm} leads to percentage variation

lower than 30% in PGA_C; the first failure always is a JF(T);

- according to EC8 2005, higher variations are observed. When f_{cm} decreases, in particular, JF(T) occurs even for gravity loads only, thus leading to a null PGA_C (i.e., $\Phi PGA_{C,50}$=0). Vice-versa, when f_{cm} increases the first failure typology becomes a beam SF;
- according to ASCE/SEI, a reduction in f_{cm} leads to very premature JF; whereas, if f_{cm} increases, joints failures disappear and the very first failure is a DF; similar outcomes are obtained according to the next generation EC8 if γ_{Rd} = 1.00 is assumed;
- according to the next generation EC8 with γ_{Rd} = 1.72, JFs(T) are very sensitive to a reduction in f_{cm}, leading to a significant PGA_C reduction due to joint failures under gravity loads only (as for EC8 2005).

For the 4-storey building, similar outcomes are obtained, except for the NTC 2018 case. In this case a f_{cm} reduction leads to considerable increments in axial load levels, and, thus, a very premature attainment of JF(C), even under vertical loads only ($\Phi PGA_{C,50}$=0). Anyway, the "reference" case (f_{cm}=20 MPa) only is analysed in what follows.

6 Retrofitting by solving shear failures

Building capacity can be improved in several ways, mainly grouped into four strategies: (i) increment of lateral strength and stiffness (e.g., by means of shear walls), (ii) increment of displacement capacity only (e.g., by fibre-reinforced polymer (FRP) wrapping or steel cages); (iii) mixed implementation of (i) and (ii); (iv) reduction of the demand (e.g., by using seismic isolators or dissipation devices). However, when shear failures significantly limit the building capacity, as in the above-analysed cases, a possible retrofitting strategy could just aim at solving the detected shear failures. This would make possible the achievement of (more favourable) ductile failures, even without any change in lateral stiffness nor in collapse mechanism. This latter retrofitting approach is one of the less invasive and less expensive strategies, and it is applied herein to analyse its effectiveness depending on the adopted code.

6.1 Retrofitting design

The main objective of the adopted strengthening strategy is the enhancement of the seismic capacity at the SD LS by solving all the (tensile-only) shear failures, without modifying the lateral stiffness of the structural elements. All details about the retrofitting design procedure can be found in De Risi et al. (2023a).

FRP wrapping (e.g., Del Vecchio et al. 2015; Pohoryles et al. 2018, 2023) is employed to mitigate shear failures in beams and columns. The number of uniaxial FRP fabrics has been designed according to CNR-DT 200/2004 guidelines. The plastic shear is used as shear demand for the design to convert shear-sensitive elements in ductile elements. The design results in a maximum number of uniaxial carbon-FRP plies (with high elastic modulus, 230 GPa, and an equivalent thickness equal to 0.166 mm) ranging from one to three. For columns, a continuous wrapping along the height is assumed. This FRP wrapping leads to an improved tensile strength ranging from 1.9 to 2.7 times the V_w (as defined in Sect. 2)

for columns, resulting in capacity-to-demand ratios ranging from 1.1 to 1.5. On the contrary, beams ending portions are wrapped (until a maximum extension of 50% of the beam length), namely only where the shear demand (assumed as plastic shear at the beams ends) overcomes the as-built shear strength. One FRP ply is always sufficient for beams, leading to capacities at least 1.8 times higher than the plastic shear load.

Pre-stressed steel strips, applied as "external stirrups", are used to effectively solve tensile shear failures in beam-column joints. The number of pre-stressed strips is designed to prevent diagonal cracking of the joint or support the maximum tensile force coming from the converging beams (Verderame et al. 2022), in tune with CEN 2005. As a result, a maximum of about twenty pre-stressed 0.9×19 mm^2 strips of stainless steel (420 MPa yielding strength) is obtained. A maximum of three holes per beam is necessary for this intervention.

Nevertheless, the adopted techniques do not allow solving the compressive failures, as defined by CEN 2005 and NTC 2018. This failure can be an issue not for beams or columns (always characterised by a tensile shear failure in the investigated buildings), but for joints (especially when characterised by high axial load levels). In other words, if a JF(C) failure occurs before the first DF (according to CEN 2005 and NTC 2018), the building capacity is limited to the first JF(C), instead than the first DF (De Risi et al. 2023a). Therefore, this intervention is intended to be applied to all shear-sensitive elements that fail during the pushover analysis up to the first DF (see Fig. 9) or the first JF(C), if any. It is also worth noting that, if JF(C) occurred for gravity loads only (as when f_{cm} is very low), such strengthening strategy would have no sense, and thus, it should be replaced with a more comprehensive and likely "heavier" retrofitting approach.

Moving towards the next-generation Eurocode, shear strength of joints strengthened with pre-stressed steel strips has been assessed based on prEN 1998-1-1:2024 and Fardis (2021), assuming that steel strips act as exterior stirrups (as for CEN 2005). Joint shear strength of (thus reinforced) joints, evaluated according to prEN 1998-1-1:2024, increases with respect to unreinforced joints, and overcomes the joint maximum shear demand for the analysed buildings. Therefore, joint shear failures result completely solved after retrofitting according to the incoming code.

Contrary to European approaches, according to ASCE/SEI, the joint transverse reinforcement is conforming if, in the joint region, the spacing of the hoops does not exceed half of the height of the column's cross-section. Therefore, it is assumed that joints strengthening - designed as described above - is able to transform non-conforming joints into conforming joints (Cosgun et al. 2019). A conforming joint has higher capacity (i.e., higher γ' coefficients in Table 1) than a relevant non-conforming joint. This leads to a higher displacement capacity (Fig. 13), and, in tune, higher $Sa_c(T_{eff})$ (Fig. 14), if compared with the *ante-operam* condition. Therefore, the *post-operam* capacity according to ASCE/SEI model is the minimum between the $Sa_c(T_{eff})$ corresponding to the first DF and that corresponding to the occurrence of a conforming joint failure.

Lastly, note also that any possible increment in column displacement capacity due to FRP wrapping is herein neglected, since it does not significantly affect the analysis of the effectiveness of the selected strengthening techniques.

6.2 Post-operam capacity assessment

Figure 13 shows the S_d capacity increments, moving from *ante-* to *post-operam* condition.

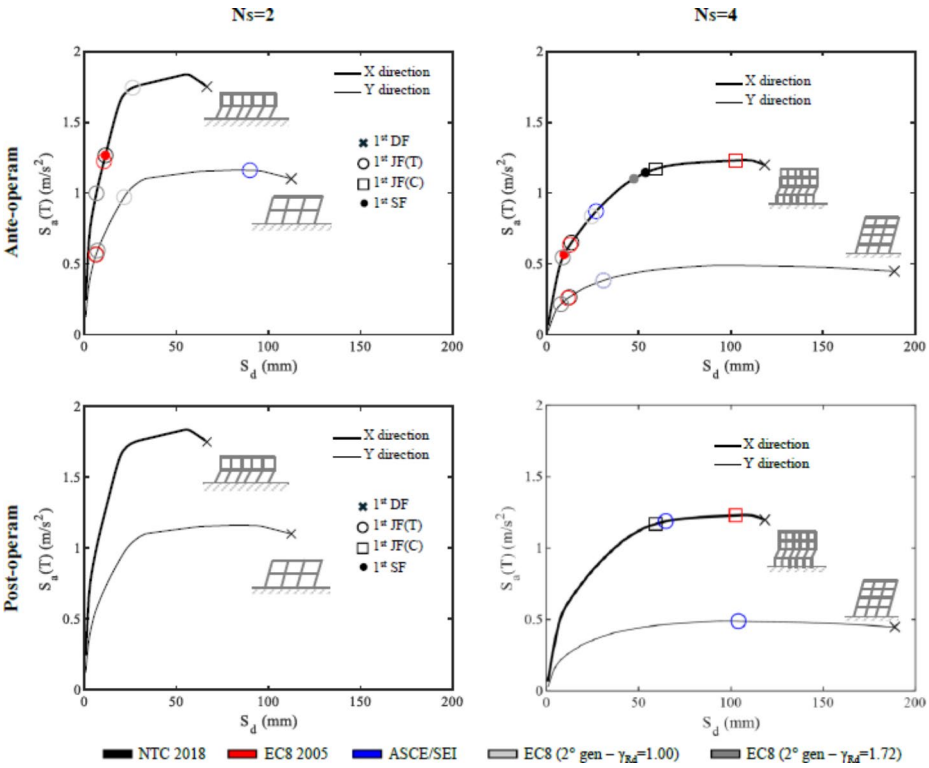

Fig. 13 Capacity curves up to the first DF with relevant brittle failures at SD LS in the post-operam condition (second row) compared to the ante-operam condition (first row)

Among current codes, the highest displacement capacity increments are observed for European/Italian codes (ranging from +83% to +94%), especially in Y direction (where no JF(C) occurs). About ASCE/SEI, displacement capacity increment reaches+60% (for Ns=4 in X direction); whereas, for Ns=2, the displacement capacity increment is null or very low since, already in as-built condition, shear failures, if any, only occur very close to the first DF.

Figure 14a shows that, for the 2-story building, after retrofit, $S_{a,\,C}(T_{eff})$ is limited by the first DF failure for all considered codes and in both directions, thus reaching the same value for all codes (Fig. 14b). The high *ante-operam* $S_{a,\,C}(T_{eff})$ according to ASCE/SEI model results in a small capacity increment in Y direction (about+20%). Vice-versa, in X direction, the ASCE/SEI-based $S_{a,\,C}(T_{eff})$ remains unchanged between the *ante-* and *post-operam* conditions, since in both conditions, the first DF defines the capacity. On the contrary, the two current Italian and European codes provide about the same $S_{a,\,C}(T_{eff})$ increment for the 2-storey building (about+85% and +95% in X and Y direction, respectively), moving from the first JF(T) to the first DF.

For the 4-storey building, the post-operam capacity is limited by the occurrence of a JF(C) in X direction according to NTC 2018 and EC8 2005, and of conforming JFs according to ASCE/SEI. The $S_{a,\,C}(T_{eff})$ in X direction according to ASCE/SEI is due to the failure of an exterior joint. On the contrary, according to European standards, the *post-operam*

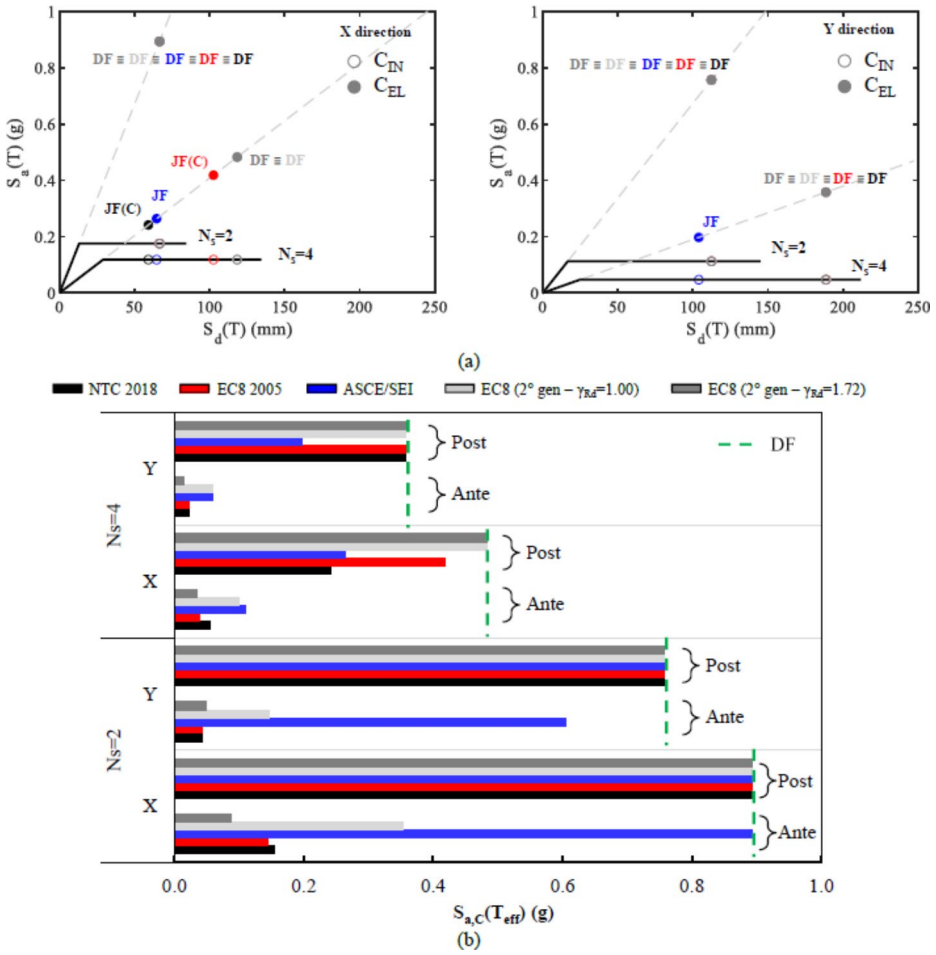

Fig. 14 Post-operam capacity in terms of $S_{a,\,C}(T_{eff})$ (**a**) and comparison with ante-operam capacity (**b**)

capacity is associated with the JF(C) of an interior joint. In this case, the highest capacity increment (among current codes) is reached with EC8 2005 capacity model (about + 90%), which allows moving from the first SF to the first JF(C). In Y direction, instead, both the current Italian and European codes provide the same $S_{a,\,C}(T_{eff})$ (corresponding to the first DF), higher than the ASCE/SEI-based $S_{a,\,C}(T_{eff})$. In this latter case, indeed, exterior (conforming) joints fail before any element reaches its ductile capacity, limiting the corresponding capacity increment (about + 65%).

Lastly, Fig. 14 also shows how the current Eurocode leads to an as-built seismic capacity quite similar to that of the future Eurocode with γ_{Rd}=1.72, in tune with observed failure evolution.

Even with the same retrofitting strategy, the resulting the *post-operam* capacity can be very different if second-generation Eurocodes is used (Fig. 14). For the 2-story building the capacity always corresponds to the first DF, thus leading to the same $S_{a,\,c}(T_{eff})$ of the previously considered current codes. Vice-versa, for the 4-storey building, the capacity provided

by the current Eurocode 8 is limited by the JF(C), contrary to what happens by using the second-generation Eurocodes in its current draft. This outcome leads to higher *post-operam* $S_{a,c}(T_{eff})$ values if the incoming code is used.

7 Conclusions

Pre-code RC buildings are particularly vulnerable to shear failures during seismic events, thus emphasizing the paramount role of a reliable estimation of shear capacity of RC elements. The scientific literature proposes different capacity models, and technical codes worldwide have significant differences as well. This study provides an overview and a comparison of shear strength models adopted by Italian, European and American codes.

About the current shear strength models for low-standard beam/column elements, a first parametric comparison found that:

- the current European standard is generally penalizing, when compared to American code;
- the model adopted by Italian code provides intermediate resistances between the European and American standards; it is derived from European one but modifies the latter for low ductility demand.

Additionally, significant differences exist in the current capacity models used to assess unreinforced beam-column joints in the European and American contexts:

- the joint resistance significantly varies with the axial load according to European and Italian models; on the contrary, in the American model, the axial load has not any role on unreinforced joint strength, which only depends on the joint geometrical configuration and the number of converging beams;
- the current European and Italian codes generally provide a lower joint resistance compared to American standard, for interior joints; for exterior joints this comparison strongly depends on axial load ratio;
- the current European and Italian models have same theoretical approach, but their hierarchy in terms of strength is strongly influenced by the joint configuration, concrete compressive strength, and axial load ratio.

All the models have been applied and compared to each other in terms of seismic capacity assessment of case-study pre-code RC buildings. They were designed for gravity loads only, with 2 or 4 stories. The assessment, at Severe Damage Limit State, based on pushover analyses, revealed that:

- the seismic capacity is severely limited by joint failures in a force-based approach for almost all buildings/codes;
- the seismic capacity in terms of elastic spectral acceleration based on the American standard overcomes that of European models (at least + 65%), while the Italian code generally falls between the other two current codes (but closely to the EC8 2005 outcome);

- an explicit modelling of the beam-column joint behaviour and a displacement-capacity safety check approach is explicitly allowed by American standard only. It leads to very less conservative results for the investigated buildings than force-based safety checks.

The incoming second generation of Eurocodes has been also investigated and applied herein based on their current available drafts and background literature. With respect to the current European standards:

- a generally less conservative safety check for beams/columns shear strength is obtained;
- a similar outcome is confirmed for beam-column intersections, mainly due to the absence of an explicit diagonal compressive safety check for unreinforced joints.

The seismic capacity of the case-study buildings was also reassessed after implementing a retrofitting strategy that addresses all tensile-only brittle failures. It was found that:

- *post-operam* capacity is due to the occurrence of the first ductile failure for the shortest building, whichever the code;
- for the tallest building, *post-operam* capacity is due to the first joint compressive failure as for the current European and Italian standards (which has always to be checked also for reinforced joints), or to a conforming joint failure as for American standard;
- the incoming shear strength model (next-generation Eurocode) for beam/column elements was found to be significantly less penalizing than the current one, thus also requiring fewer retrofitting efforts;
- the current draft of the next-generation Eurocode, unlike the current European code, leads to higher post-operam capacities. This is particularly due to the new model adopted for beam-column joints, according to which joint strength can increase with transverse reinforcement.

Buildings seismic assessment herein has been performed on 3D models neglecting infills, due to the lack of practical guidance in most codes on modelling them and the code-based framework of this study.

Nevertheless, further works, if aimed at more comprehensive fragility analysis of as-built and retrofitted buildings, should consider the paramount presence of infill panels. Lastly, it is worth noting that some further details (e.g., safety factors) have to be still defined and could somehow modify the current available versions of the second-generation Eurocodes and, thus, in this eventuality, some discussed results could be affected.

Acknowledgements This study was developed within the activities of the ReLUIS-DPC 2024–2026 research programs, funded by the Presidenza del Consiglio dei Ministri—Dipartimento della Protezione Civile (DPC).

Author contributions All authors contributed to the study conception and design. Material preparation, data collection and analysis were performed by all authors. The first draft of the manuscript was written by all authors and all authors commented on previous versions of the manuscript. All authors read and approved the final manuscript.

Funding This work was supported by Reluis-DPC project, funded by Presidenza del Consiglio dei Ministri—Dipartimento della Protezione Civile (DPC).
Open access funding provided by Università degli Studi di Napoli Federico II within the CRUI-CARE Agreement.

Declarations

Conflict of interest The authors have no relevant financial or non-financial interests to disclose.

Ethical approval All principles of ethical and professional conduct have been followed.

Informed consent Not applicable.

References

Alath S, Kunnath SK (1995) Modeling inelastic shear deformation in RC beam-column joints engineering mechanics: Proceedings of 10th Conference: University of Colorado at Boulder, Boulder, CO, May 21–24, 1995. Vol. 2. New York, NY: ASCE: 822–825

ASCE SEI/41 (2017) Seismic evaluation and retrofit of existing buildings. American Society of Civil Engineers

Baradaran Shoraka M (2013) Collapse assessment of concrete buildings: an application to non-ductile reinforced concrete moment frames (Doctoral dissertation, University of British Columbia)

Bentz EC, Vecchio FJ, Collins MP (2006) Simplified modified compression field theory for calculating shear strength of reinforced concrete elements. ACI Struct J 103(4):614

Biskinis D, Fardis MN (2010) Flexure-controlled ultimate deformations of members with continuous or lap-spliced bars. Struct Concr 11(2):93–108

Biskinis D, Fardis MN (2020) Cyclic shear resistance model for Eurocode 8 consistent with the second-generation Eurocode 2. Bull Earthq Eng 18(6):2891–2915

Biskinis DE, Roupakias GK, Fardis MN (2004) Degradation of shear strength of reinforced concrete members with inelastic cyclic displacements. Struct J 101(6):773–783

Canadian Standard Association (2006) CSA standard A23. 3–04–concrete design handbook

Celik OC, Ellingwood BR (2008) Modeling beam-column joints in fragility assessment of gravity load designed reinforced concrete frames. J Earthq Eng 12:357–381

Cirak Karakas C, Palanci M, Senel SM (2022) Fragility based evaluation of different code-based assessment approaches for the performance estimation of existing buildings. Bull Earthq Eng 20(3):1685–1716

Circolare 21/01/2019, n. 7 C.S.LL.PP. Istruzioni per l'applicazione dell'«Aggiornamento delle "Norme tecniche per le costruzioni"» di cui al decreto ministeriale 17 gennaio 2018. GU n.35 del 11-2-2019 - Suppl. Ordinario n. 5. (in Italian)

CNR-DT 200/2004 Istruzioni per la Progettazione, l'Esecuzione ed il Controllo di Interventi di Consolidamento Statico mediante l'utilizzo di Compositi Fibrorinforzati. (in Italian)

Collins MP (1978) Towards a Rational Theory for RC Members in Shear, Journal of the Structural Division, ASCE, V. 104, No. 4, Apr. pp. 649–666

Cook D, Sen A, Liel A, Basnet T, Creagh A, Koodiani HK, Smith R (2023) ASCE/SEI 41 assessment of reinforced concrete buildings: Benchmarking nonlinear dynamic procedures with empirical damage observations. Earthq Spectra 39(3):1721–1754

Cosgun C, Cömert M, Demir C, İlki A (2019) Seismic retrofit of joints of a full-scale 3D reinforced concrete frame with FRP composites. J Compos Constr 23(2):04019004

De Luca F, Verderame GM (2013) A practice-oriented approach for the assessment of brittle failures in existing reinforced concrete elements. Eng Struct 48:373–388

D.M. 2018 Aggiornamento delle Norme Tecniche per le Costruzioni - D.M. 17/1/18. (in Italian)

De Risi MT, Ricci P, Verderame GM (2017) Modelling exterior unreinforced beam-column joints in seismic analysis of non-ductile RC frames. Earthq Eng Struct Dynamics 46(6):899–923

De Risi MT, Gaudio D, C., Verderame GM (2020a) A component-level methodology to evaluate the seismic repair costs of infills and services for Italian RC buildings. Bull Earthq Eng 18(14):6533–6570
De Risi MT, Scala SA, Del Gaudio C, Verderame GM (2023a) Seismic retrofit of Italian pre-‘70 case-study RC buildings by solving shear failures: code-compliant assessment and economic effort. Int J Disaster Risk Reduct 97:104007
De Risi MT, Di Domenico M, Manfredi V, Terrenzi M, Camata G, Mollaioli F, Verderame GM (2023b) Modelling and seismic response analysis of Italian pre-code and low-code reinforced concrete buildings. Part I: bare frames. J Earthquake Eng 27(6):1482–1513
Del Gaudio C, De Risi MT, Verderame GM (2021) Seismic loss prediction for Infilled RC buildings via simplified analytical method. J Earthquake Eng, 1–34
Del Vecchio C, Di Ludovico M, Prota A, Manfredi G (2015) Analytical model and design approach for FRP strengthening of non-conforming RC corner beam–column joints. Eng Struct 87:8–20
Del Vecchio C, De Risi MT, Gaudio D, Ricci C, Di Ludovico P, M., Kang JD (2023) E-Defense 2015 ten-story building: beam–column joint assessment according to different code-based design. Bull Earthq Eng 21(15):6667–6698
Dhanvijay V, Telang D, Nair V (2015) Comparative study of different codes in seismic assessment. Comp Study Different Codes Seismic Assess 2(4):1371–1381
EN 1992-1-1:2004-12 (2004) Eurocode 2: design of concrete structures– part 1–1: General rules and rules for buildings. CEN, Brussels
EN 1998-1. CEN (2004) Eurocode 8 - design of structures for Earthquake Resistance, Part 1, General rules, seismic actions and rules for buildings. European Committee for Standardization
EN 1998-3. CEN (2005) Eurocode 8 - design of structures for Earthquake Resistance, Part 3, Assessment and Retrofitting of buildings. European Committee for Standardization
Fajfar P (2000) A nonlinear analysis method for performance-based seismic design. Earthq Spectra 16(3):573–592
Fardis MN (2021) Shear strength model for RC joints, consistent with the shear design rules for prismatic members in the second-generation Eurocodes. Bull Earthq Eng 19(2):889–917
fib Model Code (2010) Bulletin 65/66. Federation Internationale Du Beton, Lausanne: 2012, doi: 978-2-88394-105-2
FprEN 1998-1-1:2024 Eurocode 8: Design of structures for earthquake resistance—part 1–1: General rules and seismic action. Brussels: CEN; 2024
FprEN 1998-1-1:2022 Eurocode 8: Design of structures for earthquake resistance—part 1–1: General rules and seismic action. Brussels: CEN; 2022
FprEN 1992-1-1:2023 Eurocode 2: design of concrete structures—part 1–1: general rules, rules for buildings, bridges and civil engineering structures. Brussels: CEN; 2023
Franchin P, Noto F (2023) Reliability-based partial factors for seismic design and assessment consistent with second-generation Eurocode 8. Earthq Eng Struct Dynamics 52(13):4026–4047
Fujii S, Morita S (1991) CComparison between interior and exterior RC beam–column joint behavior. Design of beam–column joints for seismic resistance (SP123), American Concrete Institute: Detroit, MI, pp 145–165
Hakuto S, Park R, Tanaka H (2000) Seismic load tests on interior and exterior beam-column joints with substandard reinforcing details. Struct J 97(1):11–25
Hassan WM (2011) Analytical and experimental assessment of seismic vulnerability of beam-column joints without transverse reinforcement in concrete buildings. PhD dissertation. California, USA: University of California, Berkeley
Hassan WM, Elmorsy M (2022a) Cyclic nonlinear modeling parameters for unconfined beam-column joints. ACI Struct J 119(1):89–104
Hassan WM, Elmorsy M (2022b) Probabilistic Beam–Column Joint Model for seismic analysis of concrete frames. J Struct Eng 148(4):04022011
ISTAT (2011) Istituto Nazionale di Statistica (National Institute of Statistics). 15° Censimento generale della popolazione e delle abitazioni. Dati sulle caratteristiche strutturale della popolazione, delle abitazioni e variabili (2011). (in Italian)
Jeon JS, Shafieezadeh A, DesRoches R (2014) Statistical models for shear strength of RC Beam-column joints using machine-learning techniques. Earthq Eng Struct Dynamics 43(14):2075–2095
Kim J, LaFave JM (2012) A simplified approach to joint shear behavior prediction of RC Beam-column connections. Earthq Spectra 28(3):1071–1096
Kowalsky MJ, Priestley MN (2000) Improved analytical model for shear strength of circular reinforced concrete columns in seismic regions. Struct J 97(3):388–396
Li B, Siu-Shu Lam E, Wu B, Wang YY (2015) Effect of high Axial load on seismic behavior of Reinforced concrete Beam-Column joints with and without strengthening. ACI Struct J 112(6)

Lupoi G, Calvi GM, Lupoi A, Pinto PE (2004) Comparison of different approaches for seismic assessment of existing buildings. J Earthquake Eng 8(spec01):121–160
Maranhão H, Varum H, Melo J, Correia AA (2024) Comparative analysis of the impact of design and detailing provisions for RC moment resisting frames under the first-and second-generation of Eurocode 8. Eng Struct 306:117809
Marcantonio PR, Ožbolt J, Petrangeli M (2015) Rational approach to prediction of shear capacity of RC Beam-column elements. J Struct Eng 141(2):04014104
Masi A, Chiauzzi L, Santarsiero G, Manfredi V, Biondi S, Spacone E, Verderame GM (2019) Seismic response of RC buildings during the M w 6.0 August 24, 2016 Central Italy earthquake: the Amatrice case study. Bull Earthq Eng 17:5631–5654
McKenna F (2011) OpenSees: a framework for earthquake engineering simulation. Comput Sci Eng 13(4):58–66
Mörsch E (1909) Concrete-steel construction:(Der Eisenbetonbau). Engineering news publishing Company
NZS 3101 (2006) Concrete structures standards, vols. 1 and 2. Standards Association of New Zealand
Pantelides CP, Clyde C, Reaveley LD (2002) Performance-based evaluation of reinforced concrete building exterior jointsfor. Seismic Excitation Earthq Spectra 18(3):449–480
Park S, Mosalam KM (2012) Parameters for shear strength prediction of exterior beam–column joints without transverse reinforcement. Eng Struct 36:198–209
Paulay T, Priestley MJN (1992) Seismic design of reinforced concrete and masonry buildings. Wiley Interscience
Pohoryles DA, Melo J, Rossetto T, D'Ayala D, Varum H (2018) Experimental comparison of novel CFRP retrofit schemes for realistic full-scale RC beam–column joints. J Compos Constr 22(5):04018027
Pohoryles DA, Minas S, Melo J, Bournas DA, Varum H, Rossetto T (2023) A novel FRP retrofit solution for improved local and global seismic performance of RC buildings: development of fragility curves and comparative cost-benefit analyses. J Earthquake Eng 1–19
prEN 1998-3:2023 Eurocode 8: Design of structures for earthquake resistance - Part 3: Assessment and retrofitting of buildings and bridges. Brussels: CEN; 2023
Priestley MJN (1997) Displacement-based seismic assessment of reinforced concrete buildings. J Earthquake Eng 1(01):157–192. https://doi.org/10.1142/S1363246997000088
Priestley MJN, Verma R, Xiao Y (1994) Seismic shear strength of reinforced concrete columns. J Struct Eng ASCE 120(8):2311–2329
R.D. Regio Decreto Legge n. 2229 Del 16/11/1939. Norme per la esecuzione delle opere in conglomerate cementizio semplice Od Armato. G.U. n. 92 Del 18/04/1940 (in Italian).
Ritter W (1899) Die bauweise hennebique (hennebiques construction method)
Sen A, Cook D, Liel A, Basnet T, Creagh A, Khodadadi Koodiani H, Smith R (2023) ASCE/SEI 41 assessment of reinforced concrete buildings: Benchmarking linear procedures and FEMA P-2018 with empirical damage observations. Earthq Spectra 39(3):1658–1682
Sezen H, Moehle JP (2004) Shear strength model for lightly reinforced concrete columns. J Struct Eng 130(11):1692–1703
TBEC-2018 (2018) Türkiye building earthquake code, Republic of Türkiye Ministry of Interior Disaster and Emergency Management Authority, Ankara
Tsonos AG (2007) Cyclic load behavior of reinforced concrete beam–column subassemblages of modern structures. ACI Struct J 104(4):468–478
Vecchio FJ, Collins MP (1986) The modified compression-field theory for reinforced concrete elements subjected to shear. ACI J 83(2):219–231
Verderame GM, Ricci P (2018) An empirical approach for nonlinear modelling and deformation capacity assessment of RC columns with plain bars. Eng Struct 176:539–554
Verderame GM, Polese M, Mariniello C, Manfredi G (2010) A simulated design procedure for the assessment of seismic capacity of existing reinforced concrete buildings. Adv Eng Softw 41(2):323–335
Verderame GM, Ricci P, De Luca F, Del Gaudio C, De Risi MT (2014) Damage scenarios for RC buildings during the 2012 Emilia (Italy) earthquake. Soil Dyn Earthq Eng 66:385–400
Verderame GM, Ricci P, De Risi MT, Del Gaudio C (2022) Experimental response of unreinforced exterior RC joints strengthened with prestressed steel strips. Eng Struct 251:113358
Vidic T, Fajfar P, Fischinger M (1994) Consistent inelastic design spectra: strength and displacement. Earthq Eng Struct Dynamics 23(5):507–521
Vollum RL, Newman JB (1999) Strut and tie models for analysis/design of external beam–column joints. Mag Concr Res 51(6):415–425